Concurrent Operation of Wireless Power Transfer Based Contactless Slip Ring and Motor Drive System with a Single Converter

Enes Ayaz

M.Sc. Thesis Defense

Middle East Technical University (METU), Department of Electrical and Electronics Engineering Ankara, TURKEY

September 2022

Outline

1. Aim of Study
2. Wireless Power Transfer System Basics
3. Theory Of Operations
4. Implementation for DC Motor
5. Implementation for AC Motor
6. Implementation for field excitation
7. Conclusion

Power Transfer to Rotating Frames

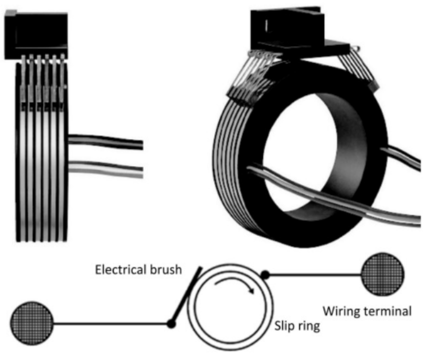

Slip Rings

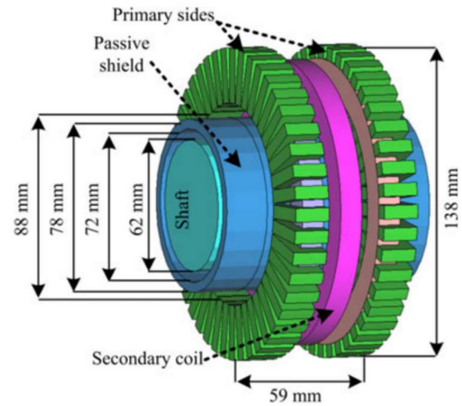

Contactless

Slip Rings

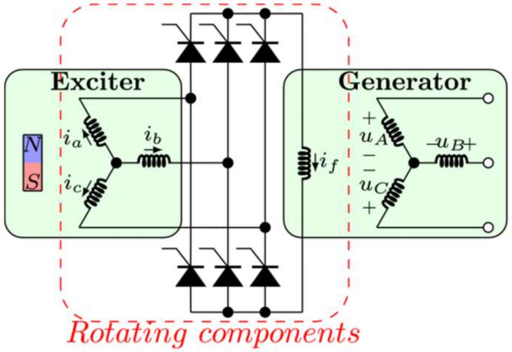

Brushless Exciter

Power Transfer to Rotating Frames

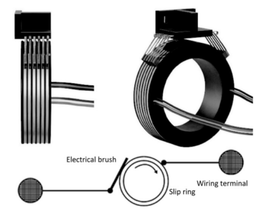

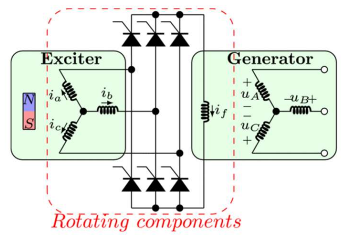

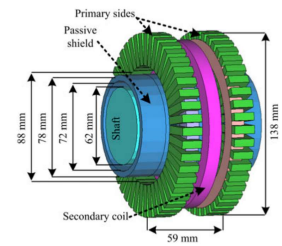

	Slip Rings	Brushless Exciters	Contactless Slip Rings
Reliability	-	+	+
Maintenance	-	+	+
Simplicity	+	+	-
Speed Independency	+	-	+
Cost Effectivity	+	+	-
Efficiency	+	-	+

Wireless Power Transfer Based Contactless Slip Rings

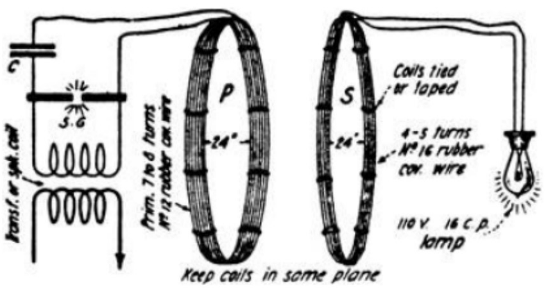

Tesla's WPT System

	Inductive Power Transfer	Capacitive Power Transfer
Transfer Type	Varying MF	Varying EF
Power Ratings	High	Low
Frequencies	Low	High
Efficiency	High	High
Distance	Moderate	Low

Inductive Power Transfer

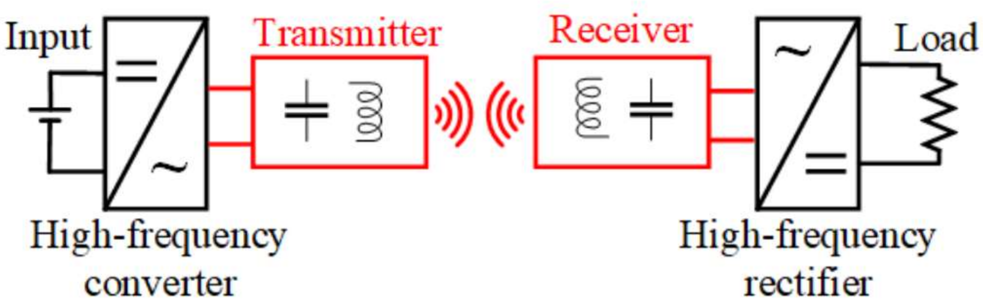

1. DC/AC converter
2. Compensation Circuits
3. Transmitter/Receiver Coils
4. AC/DC Rectifiers

Conventional Inductive Power Transfer Based Contactless Slip Ring

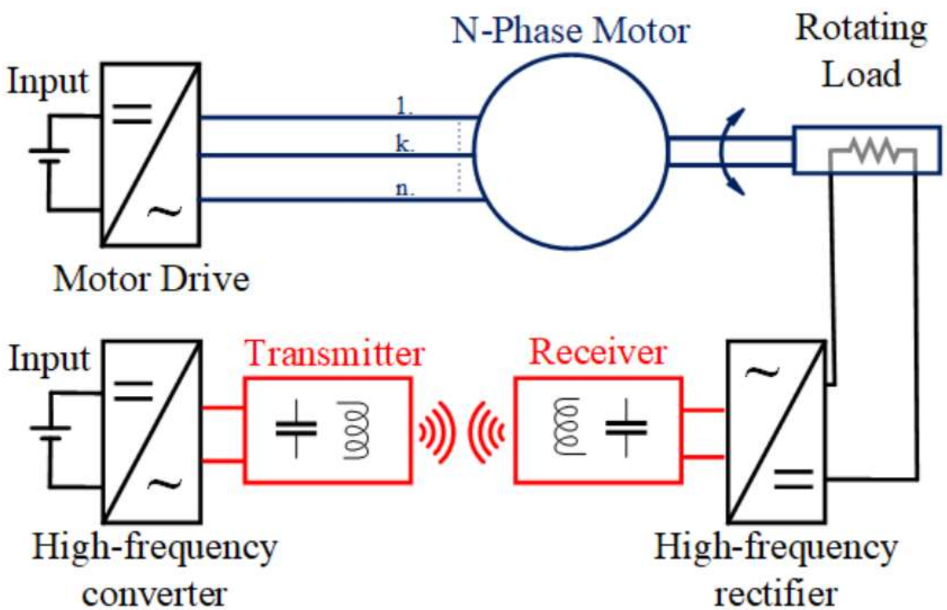

Two converters:

1. To drive the motor
2. To excite the Tx coil

Motor → attenuated in motor current

The motor drive → generating low and high frequency

Motor → used to drive

The WPT converter → generating high frequency

The WPT system →behaves like band-pass filter

Proposed Inductive Power Transfer Based Contactless Slip Ring

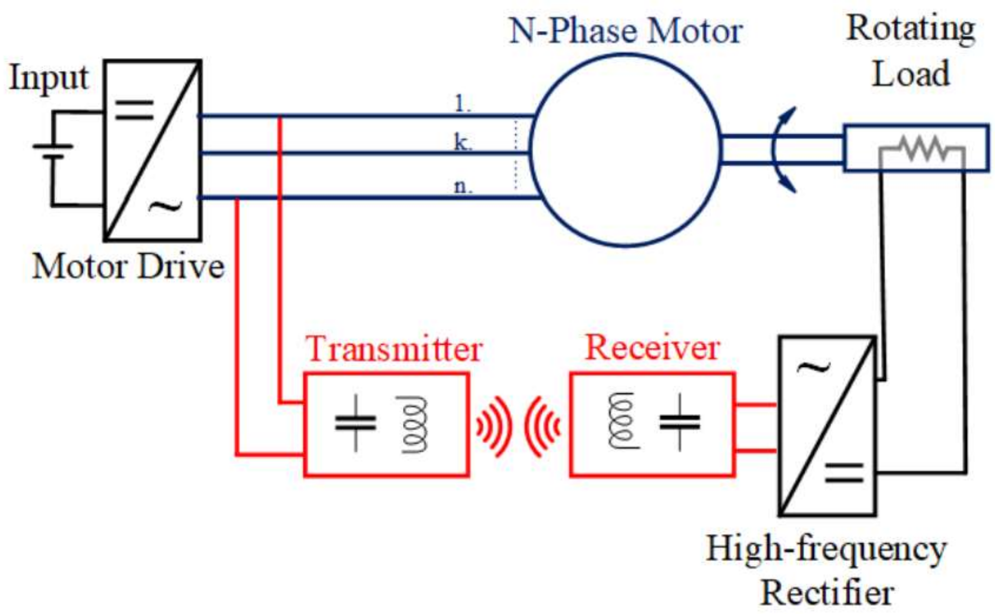

The motor drive → generating high frequency

combining ↓

The WPT system →behaves like band-pass filter

eliminating ↓

~~The WPT converter → generating high frequency~~

Proposed Inductive Power Transfer Based Contactless Slip Ring

	Conventional Contactless Slip Ring	Proposed Contactless Slip Rings
Reliability	+	+
Maintenance	+	+
Simplicity	-	+
Speed Independency	+	+
Cost Effectivity	-	+
Efficiency	+	+

METU POWER LAB

Outline

Inductive Power Transfer System

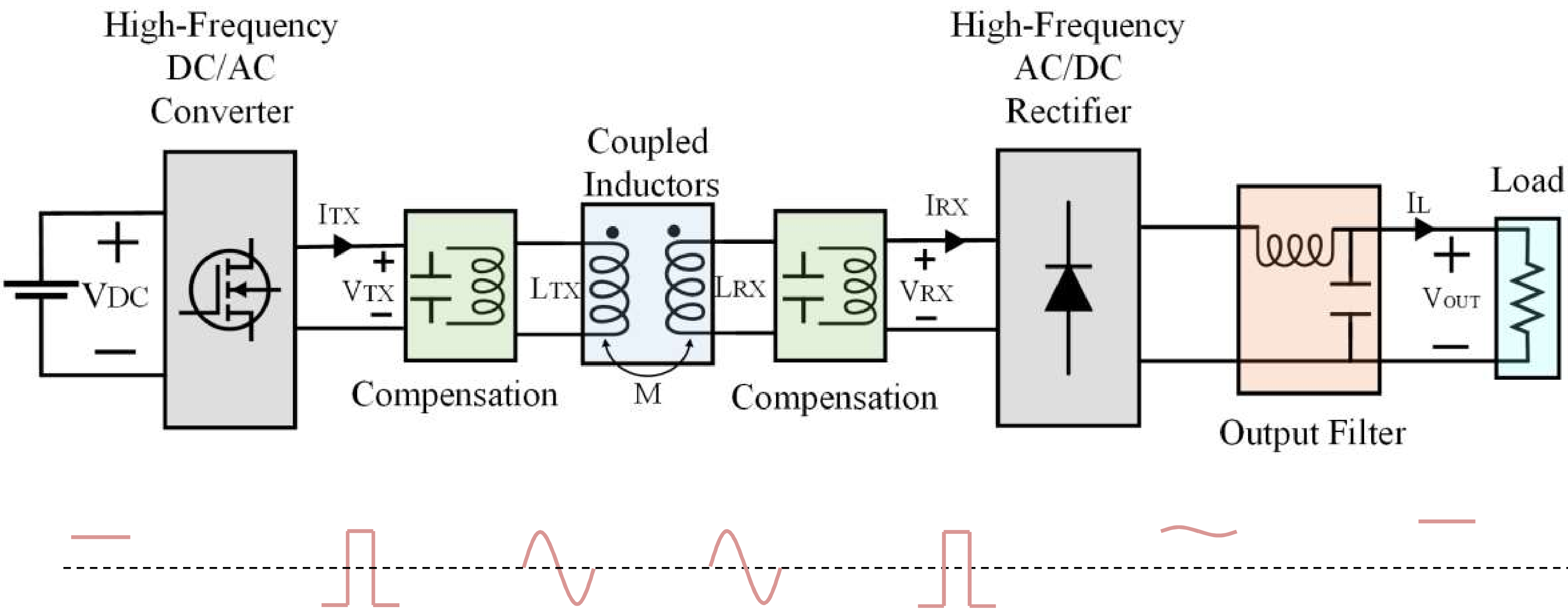

METU POWER LAB

Compensation Topologies

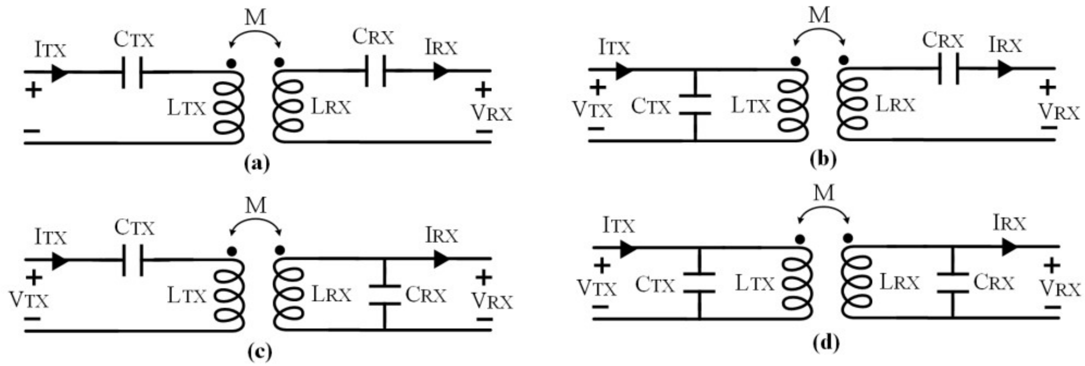

a) Series-series
b) Parallel-series
c) Series-parallel
d) Parallel-parallel

Series-Series Compensation	
Source Type	Voltage Source
Resonant frequency	Load Independent
Resonant frequency	Coupling Independent
No load operation	Short Circuit
Capacitor Size	Large

Series-Series IPT System

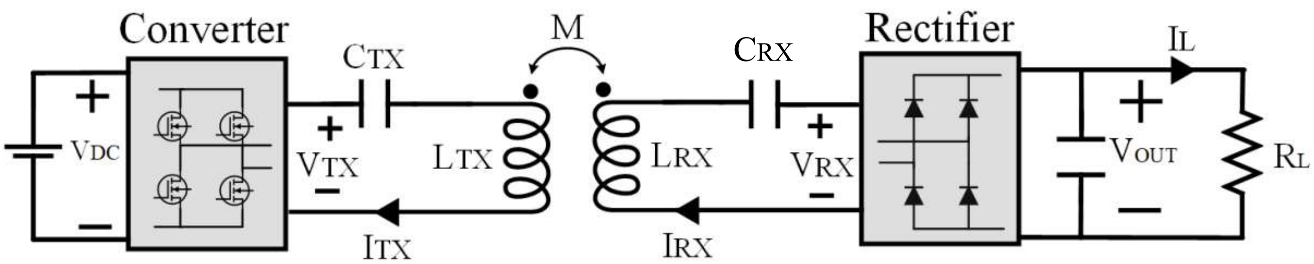

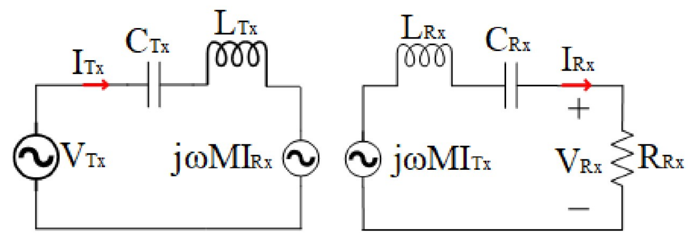

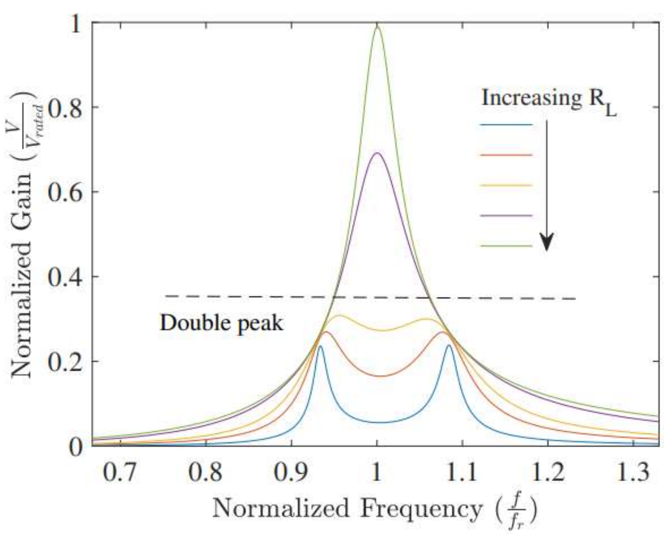

Single-peak band pass filter

↓

First Harmonic Approach (FHA)

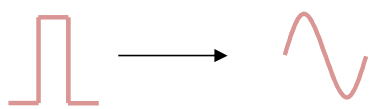

Phase < 0 → Inductive region

$f_{op} > f_r$ → Inductive region

$$f_r = \frac{1}{\sqrt{L_{Tx}C_{Tx}}} = \frac{1}{\sqrt{L_{Rx}C_{Rx}}}$$

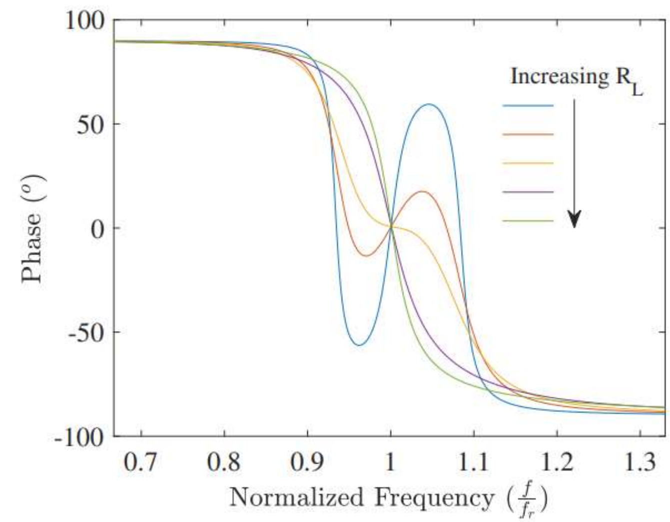

Zero Voltage Switching

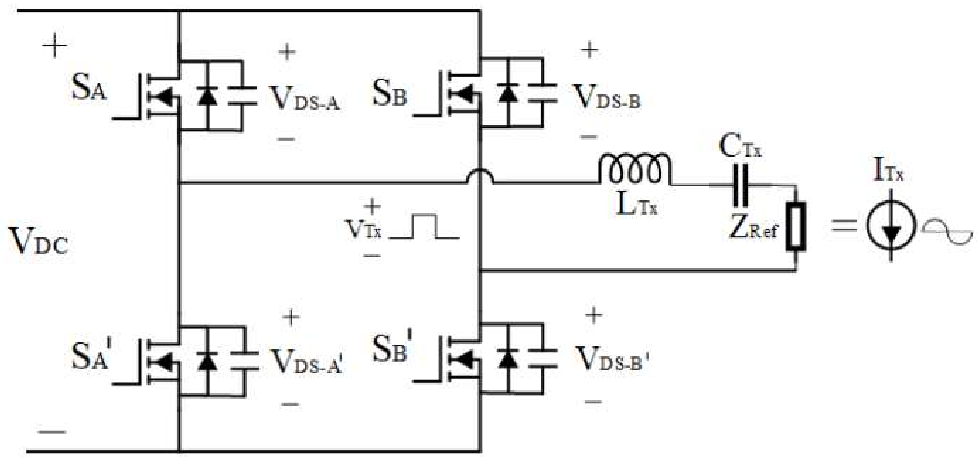

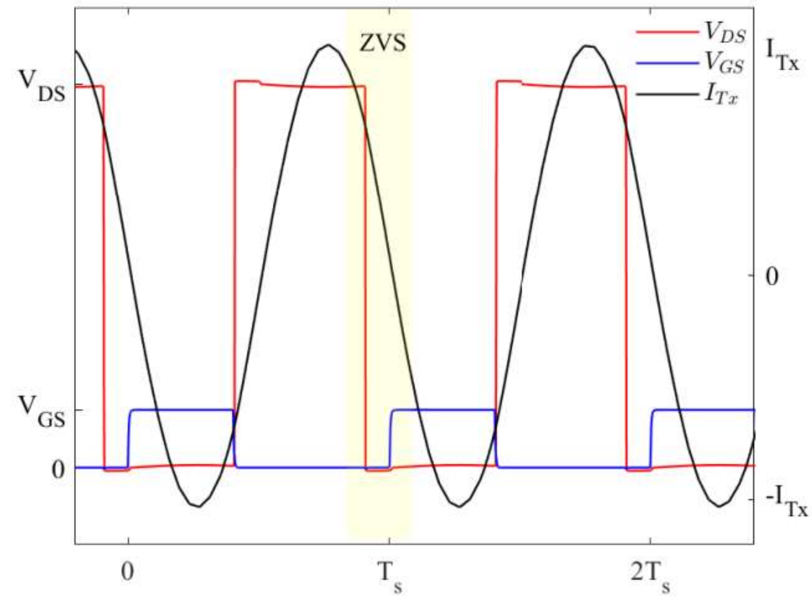

Inductive region → The capacitance of the switches discharges by the load current during dead time.

Bifurcation Phenomenon

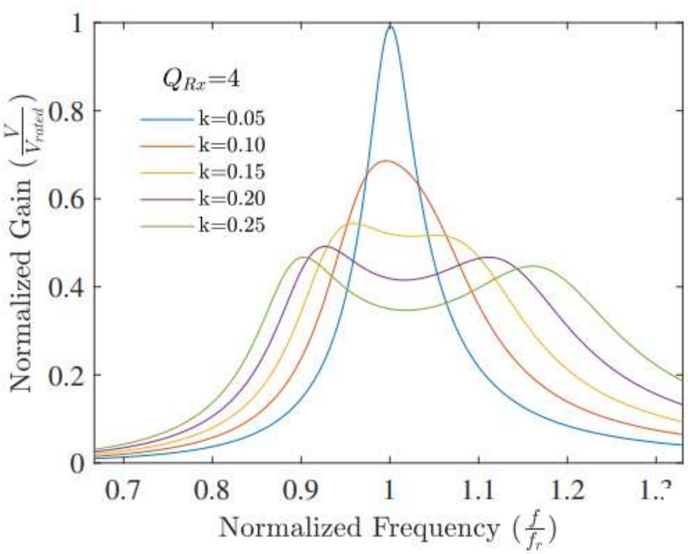

Double-peak

↓

~~$f_{op} > f_r$ → Inductive region~~

↓

- Making control difficult
- Decreasing efficiency

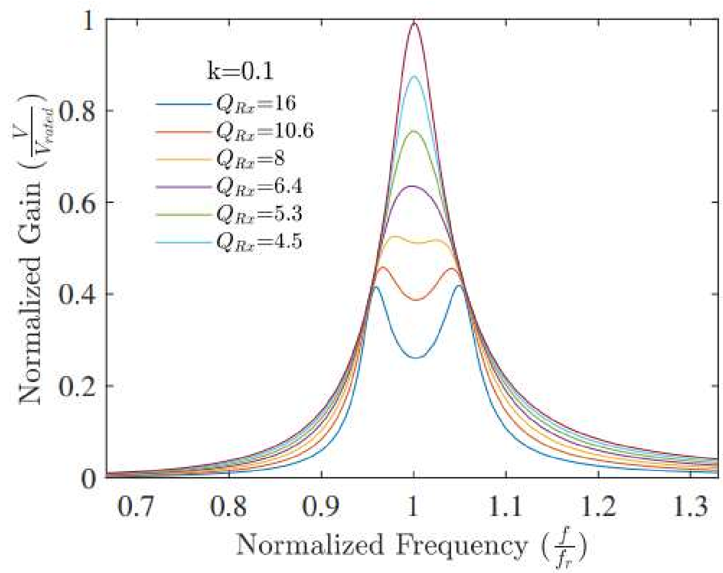

$$k_c = \frac{1}{Q_{Rx}}\sqrt{1 - \frac{1}{4Q_{Rx}^2}}$$

Multifrequency IPT Systems

Aims:

1. To Increase power
2. To reduce switching components
3. To increase DC-link utilization rate
4. Operating in more than one standards

Studies:

1. Multi-converter and multi-resonant
2. Single-converter and multi resonant
3. Single-converter and multi-load

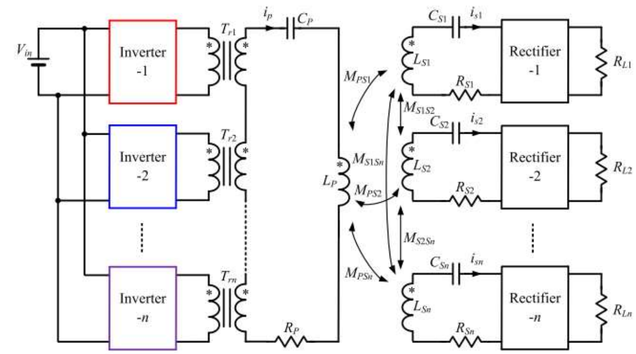

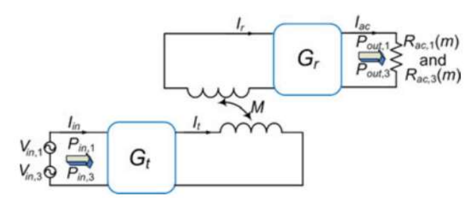

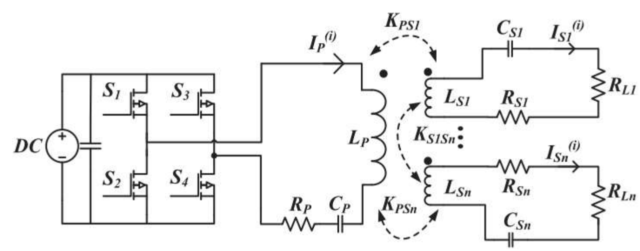

Outline

1. Aim of Study
2. Inductive Power Transfer System Basics
3. **Theory Of Operations**
4. Implementation for DC Motor
5. Implementation for AC Motor
6. Implementation for field excitation
7. Conclusion

The Proposed Contactless Slip Ring Method

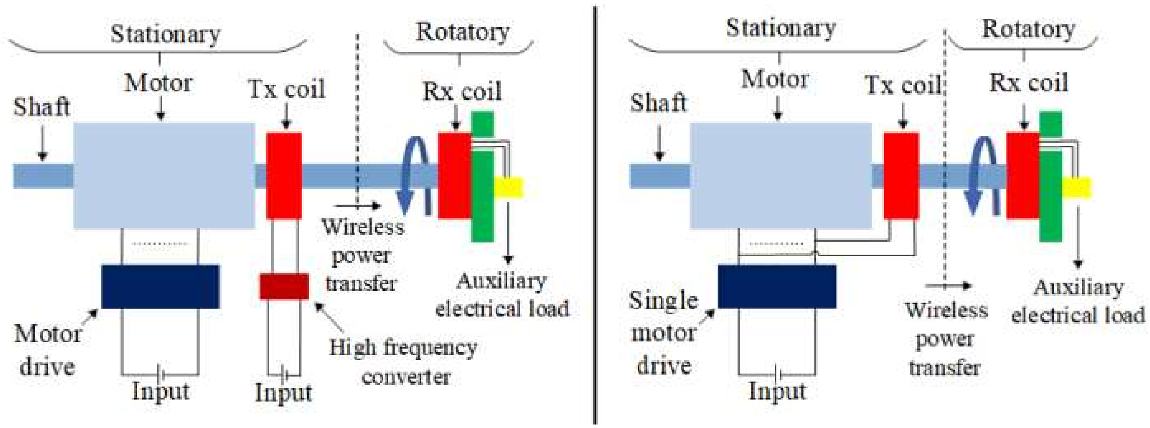

Conventional System Proposed System

Motor Drives

- DC motor drive
- AC motor drive

DC Motor Drives

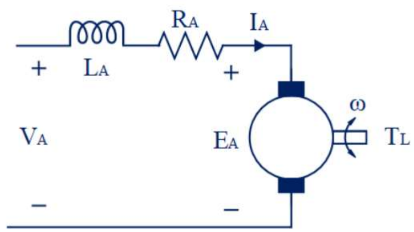

Varying armature voltage

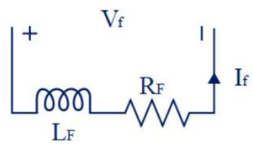

Constant field excitation

$$E_a = K_A \omega$$

$$T = K_A I_A$$

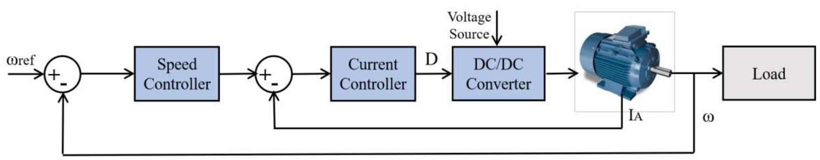

Control diagram

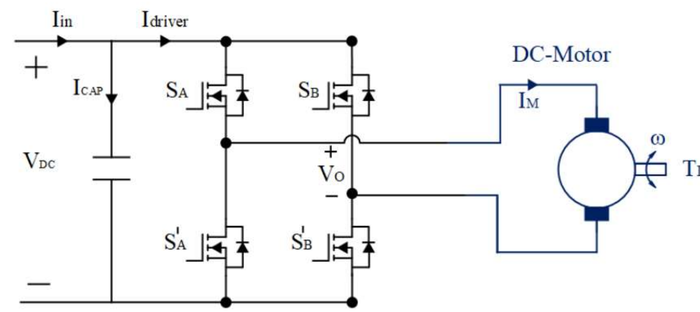

Full-Bridge Converter

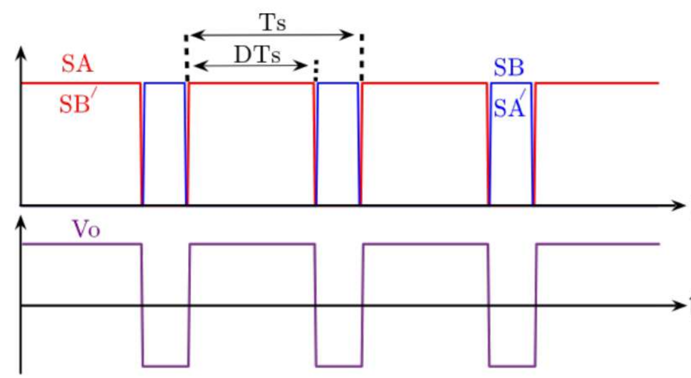

METU POWER LAB

Proposed Modulation Technique

$$S(t) = \mathrm{D} + \sum_{\mathrm{k}=1}^{\infty} \frac{2}{\mathrm{k}\pi} \sin(\mathrm{k}\pi \mathrm{D}) \cos(2\pi \mathrm{k} \mathrm{f_s} \mathrm{t})$$

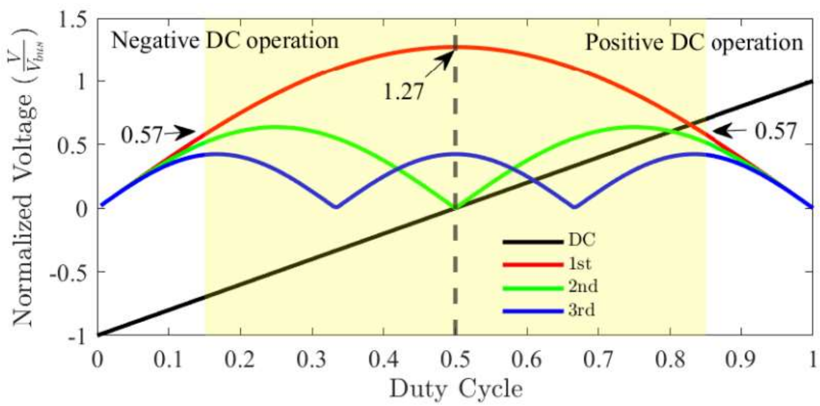

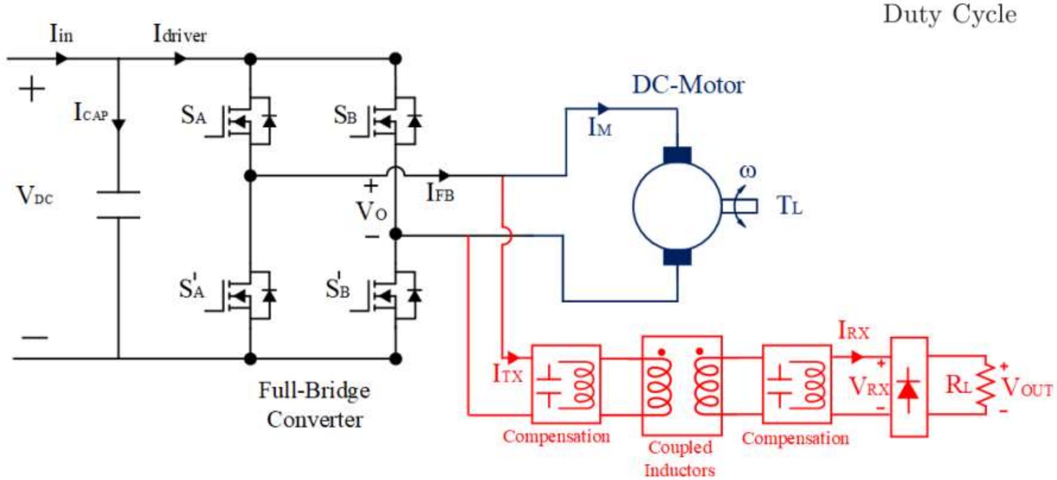

Proposed Control Method

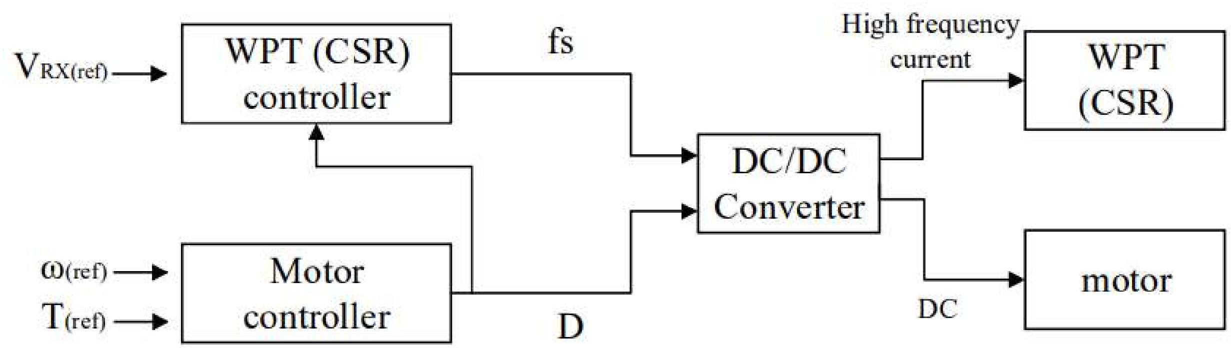

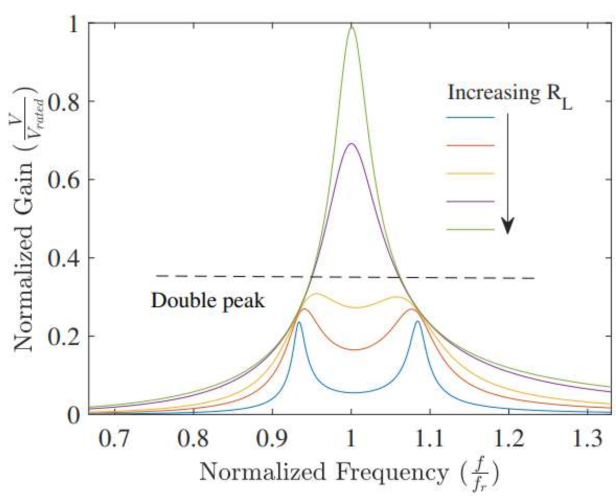

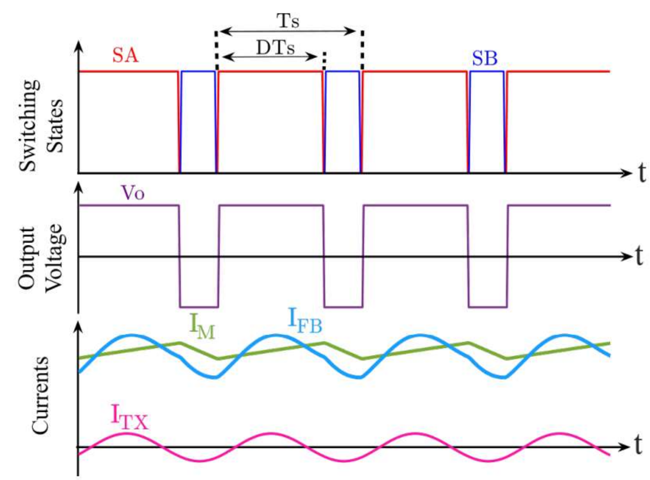

AC Motor Drives

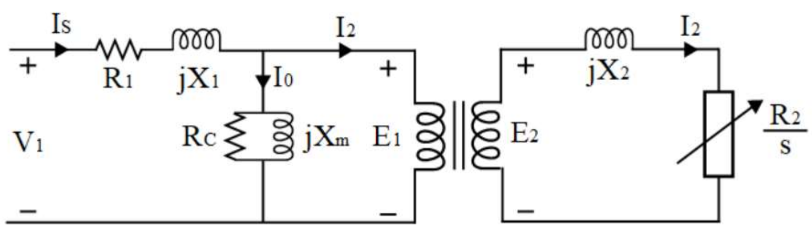

Induction motor

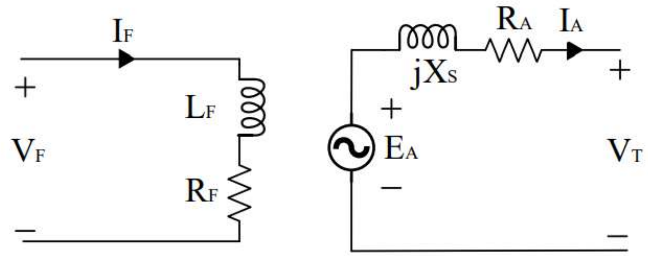

Synchronous motor

Varying armature voltage and frequency

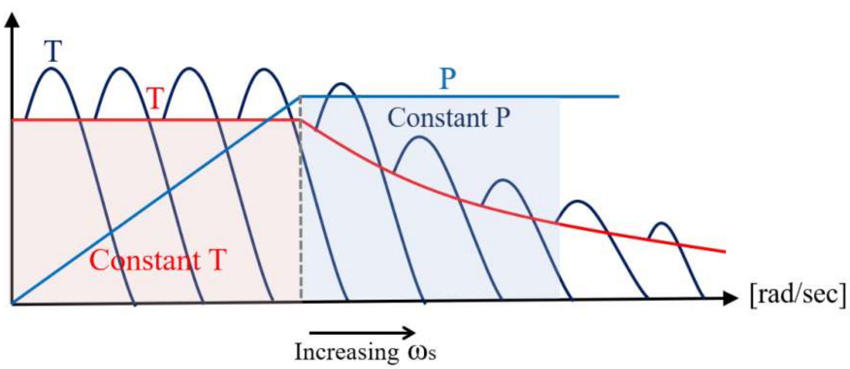

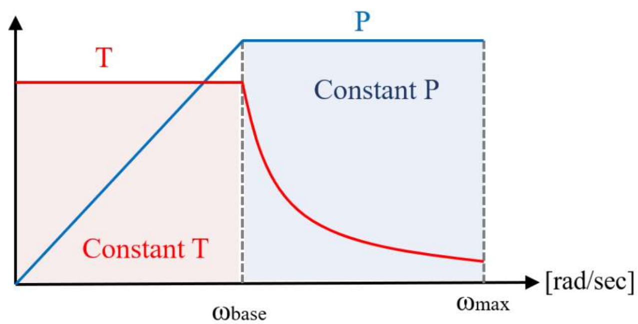

METU Power Lab

Conventional Modulation Technique

$$
\begin{aligned}
S = {} & \frac{1}{2} + \frac{m_a}{2}\cos\left(\omega_o t + \theta_o\right) \\
& + \frac{2}{\pi}\sum_{i=1}^{i=\infty} J_o\left(i\frac{\pi}{2}m_a\right)\sin\left(i\frac{\pi}{2}\right)\cos\left(i(\omega_c t + \theta_c)\right) \\
& + \frac{2}{\pi}\sum_{i=1}^{i=\infty}\sum_{k=-\infty}^{k=\infty}\left(\begin{array}{c} \frac{1}{i}J_k\left(i\frac{\pi}{2}m_a\right)\sin\left((i+k)\frac{pi}{2}\right) \\ \cos\left(i(w_c t + \theta_c) + k(w_o t + \theta_o)\right) \end{array}\right)
\end{aligned}
$$

Frequency	**Leg A**	**Leg B**	**Leg C**	**Sequence**
f_o	0^o	120^o	-120^o	Positive
$f_s - 2f_o$	0^o	120^o	-120^o	Positive
f_s	0^o	0^o	0^o	Zero
$f_s + 2f_o$	0^o	-120^o	120^o	Negative

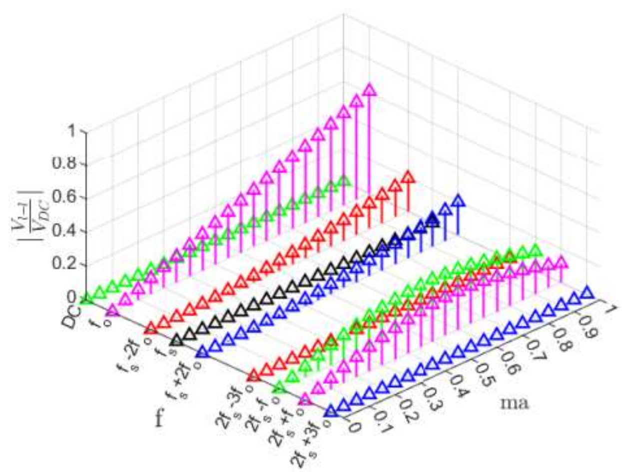

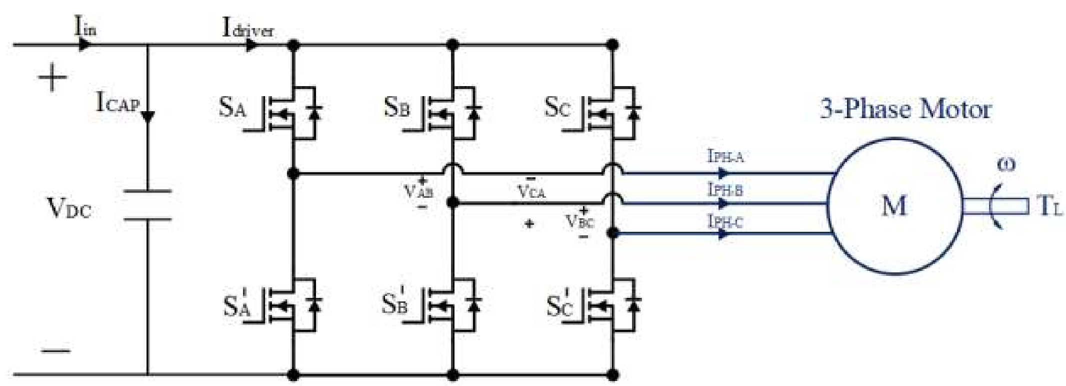

3-Wire 3-Phase Inverter

Proposed Modulation Technique

$$Carrier\ phases \begin{cases} \phi_{cA} = 0 \\ \phi_{cB} = \phi_{CPS} \\ \phi_{cC} = 0 \end{cases}$$

$$V_{sl}(m_a) = \frac{2}{\pi} J_2\left(m_a \frac{\pi}{2}\right) \sqrt{1 - cos(\phi_{CPS} + 120^o)}$$

$$V_s(m_a) = \frac{2}{\pi} J_o\left(m_a \frac{\pi}{2}\right) \sqrt{1 - cos(\phi_{CPS})}$$

$$V_{sh}(m_a) = \frac{2}{\pi} J_2\left(m_a \frac{\pi}{2}\right) \sqrt{1 - cos(\phi_{CPS} - 120^o)}$$

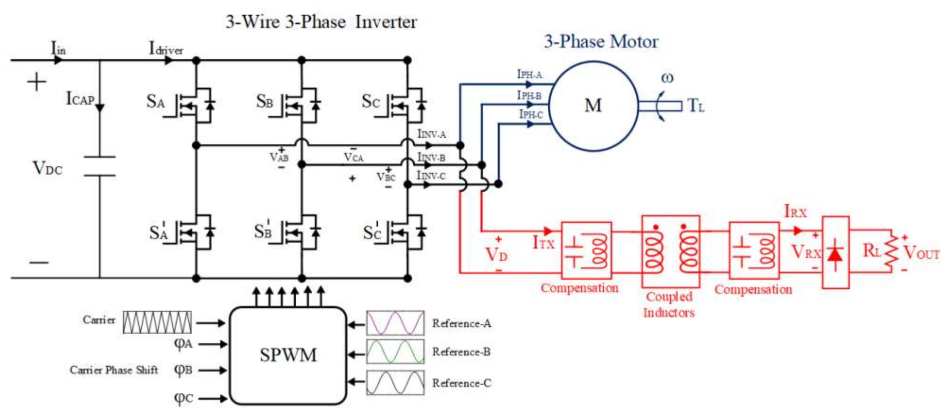

Proposed Modulation Technique

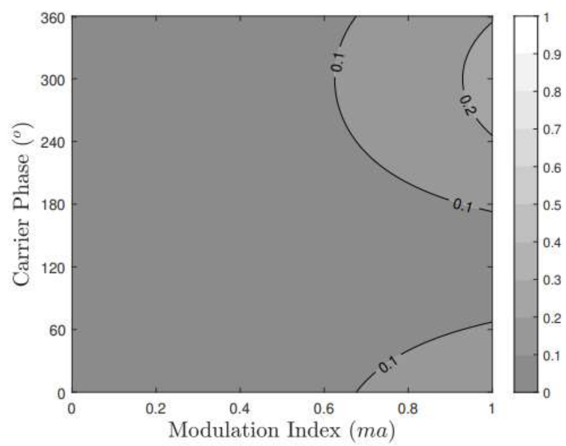

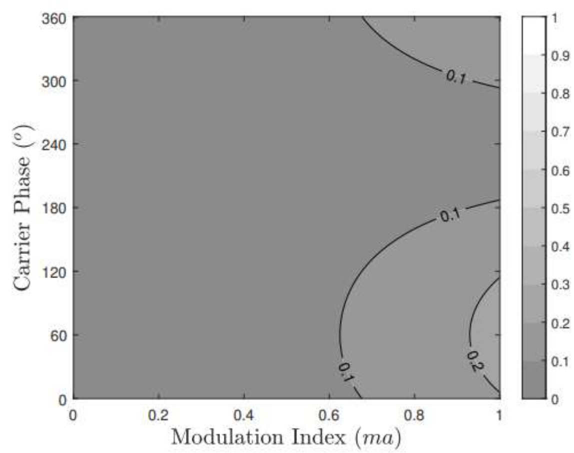

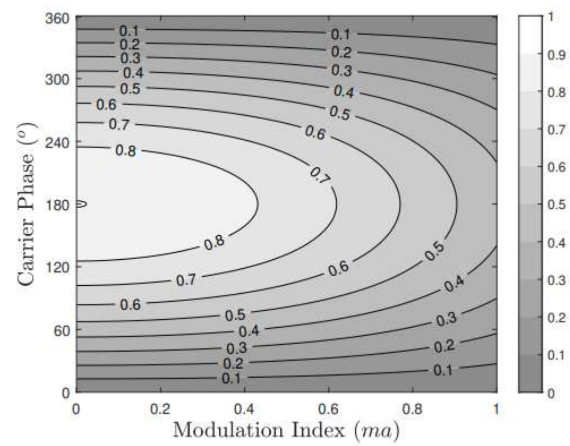

$$V_D = \sqrt{\left(V_{sl}^2 + V_{sw}^2 + V_{sh}^2\right)}$$

Proposed Control Method

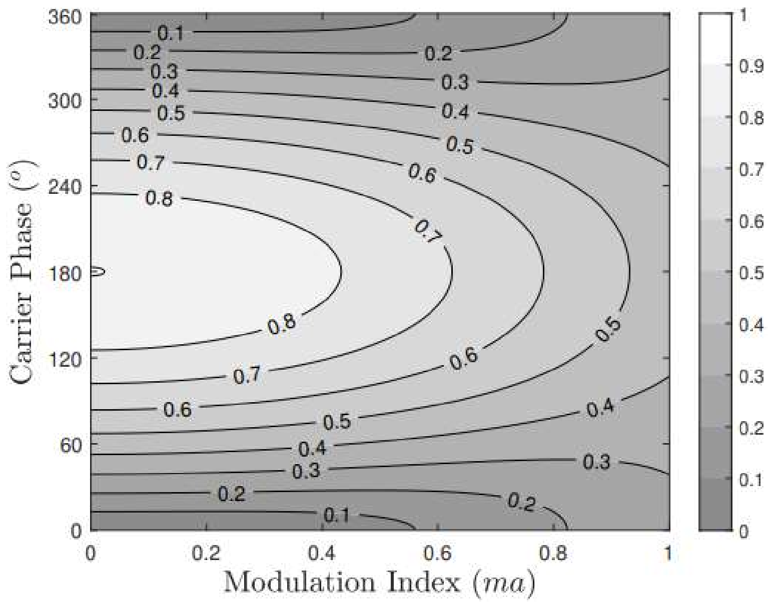

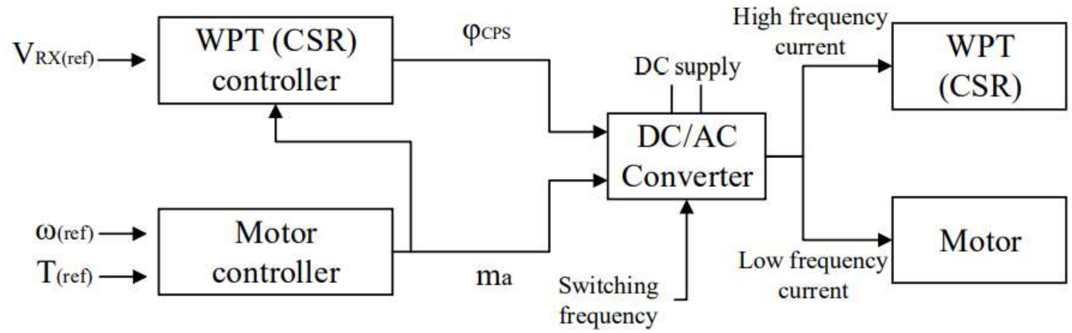

Practical Considerations

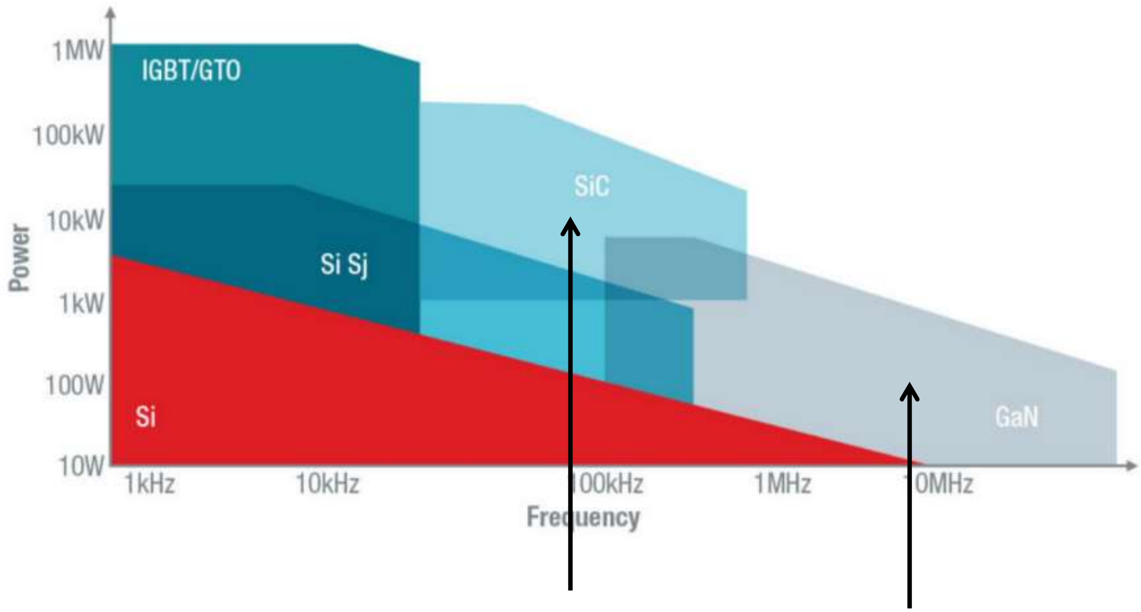

WPT systems $\xrightarrow{\text{require higher switching frequency}}$ smaller coil sizes

Motor drives $\xrightarrow{\text{require lower switching frequency}}$ to reduce switching losses

Both requirements are provided GaN or SiC based motor drives

Outline

1. Aim of Study
2. Inductive Power Transfer System Basics
3. Theory Of Operations
4. **Implementation for DC Motor**
5. Implementation for AC Motor
6. Implementation for field excitation
7. Conclusion

System Overview and Experimental Setup

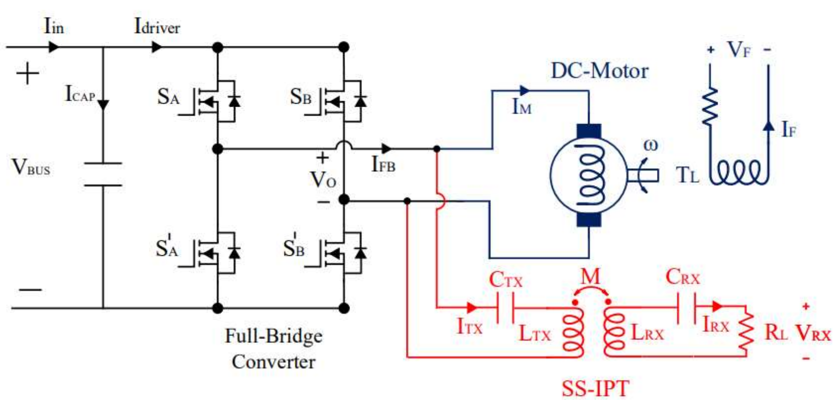

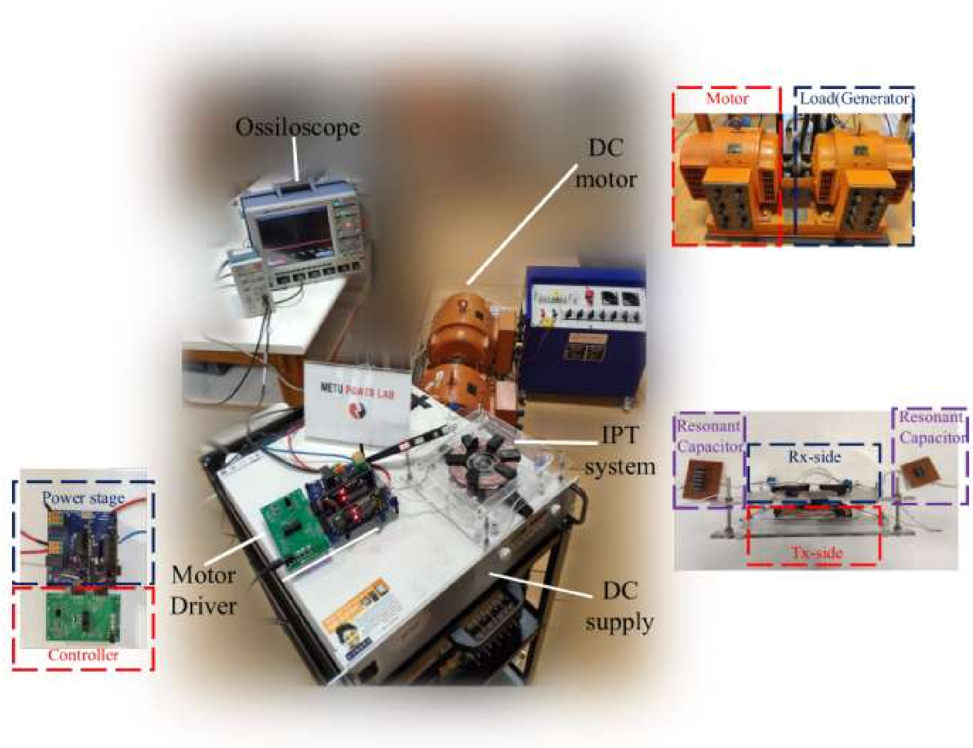

Wireless Power Transfer System Design

The Rated Voltages and Powers	
Input Voltage (V_{BUS})	100 V_{DC}
IPT Output Voltage (V_{RX})	20 V_{RMS}
Motor Output Power (P_M)	500 W
IPT Output Power (P_o)	50 W

The Motor Parameters	
Armature resistance (R_a)	2 Ω
Armature inductance (L_a)	7 mH
Motor electrical time constant (T_s)	3.5 ms

The Drive Parameters	
Duty cycle(D)	$0.15 - 0.85$
Switching frequency (f_s)	$<$ 100 kHz
Switching period (T_s)	$>$ 10 μs

$$V_{o,1^{st}}(rms) = \frac{4}{\sqrt{2}\pi} V_{Bus} sin(\pi D)$$

$$\downarrow$$

$$0.15 < D < 0.85$$

$$40\ V_{RMS} < V_{o,1^{st}}(rms) < 90\ V_{RMS}$$

$$Q_{RX} \longrightarrow \mathrm{L_{RX}} = \frac{\mathrm{Q_{RX} R_L}}{\omega_\mathrm{o}} \longrightarrow \mathrm{M} = \frac{\mathrm{V_{RX} V_{o,1^{st}}}}{\mathrm{P_o}\omega_\mathrm{o}}$$

$$\downarrow$$

$$\mathrm{C_{TX,RX}} = \frac{1}{\mathrm{L_{TX,RX}}}\omega_\mathrm{o}^2 \longleftarrow \mathrm{L_{TX}} = \frac{\mathrm{V^2_{o,1^{st}}}}{\mathrm{k^2}\omega_\mathrm{o}^2 \mathrm{Q_{RX}}} \longleftarrow k$$

Wireless Power Transfer System Design

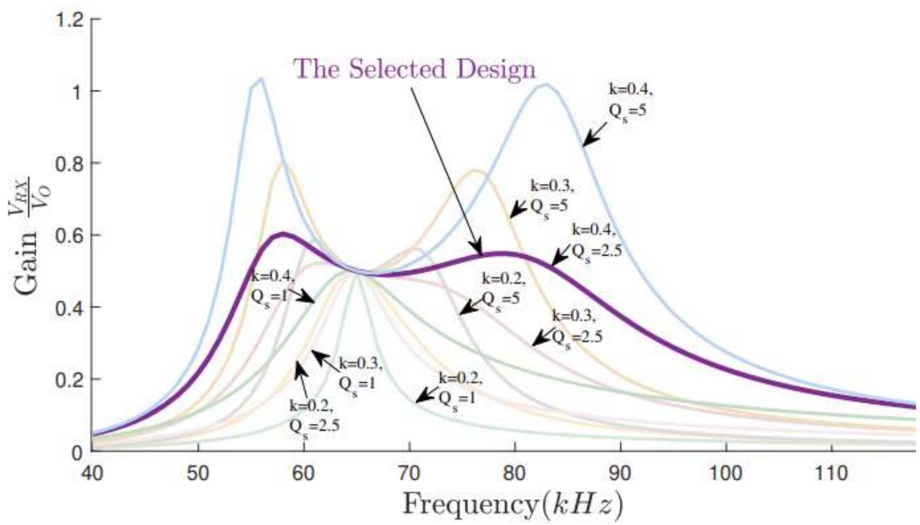

Receiver quality factor (Q_{RX})	2.6
Resonant frequency (f_0)	65 kHz
Coupling factor (k)	0.40
Load resistance (R_L)	8 Ω
Receiver coil inductance (L_{RX})	51 μH
Mutual inductance (M)	41 μH
Transmitter coil inductance (L_{TX})	205 μH
Receiver resonant capacitance (C_{TX})	115 nF
Transmitter resonant capacitance (C_{RX})	29 nF
Voltage gain at f_o	0.5

Coil Design

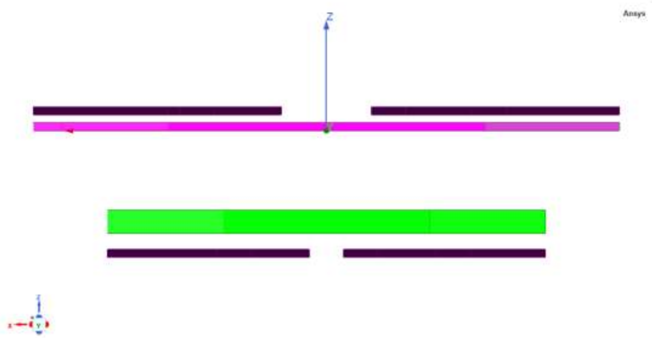

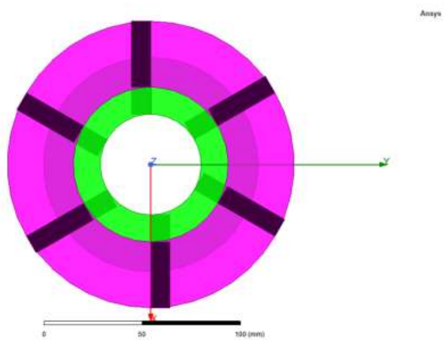

Tx-coil inner diameter	52 mm
Tx-coil outer diameter	110.6 mm
Tx number of layer	3
Tx conductor diameter	2 mm
Tx-coil total turns/turns per layer	44/15
Rx-coil inner diameter	80 mm
Rx-coil outer diameter	148 mm
Rx conductor diameter	2 mm
Rx-Coil total turns/turns per layer	17/17
Airgap	20 mm
Tx-coil inductance	204 μH
Rx-coil inductance	52 μH
Mutual inductance	41 μH

Impedance Modelling and Control

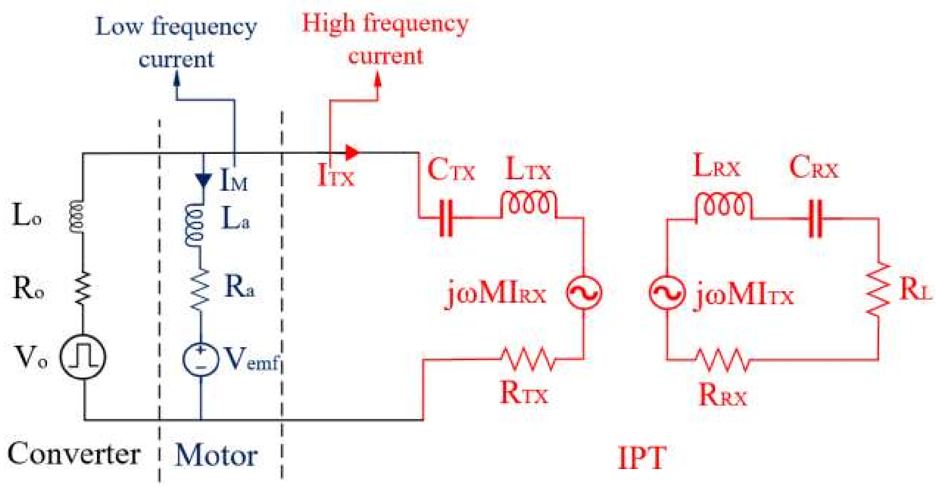

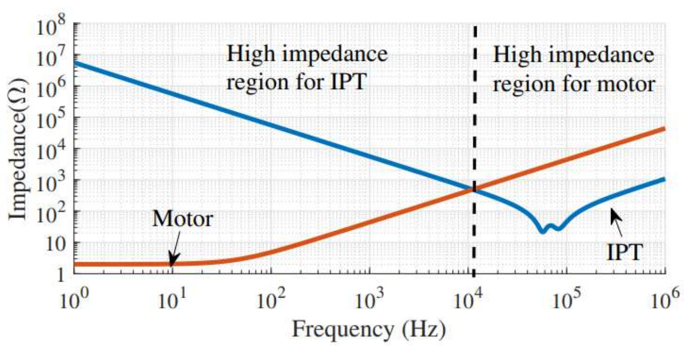

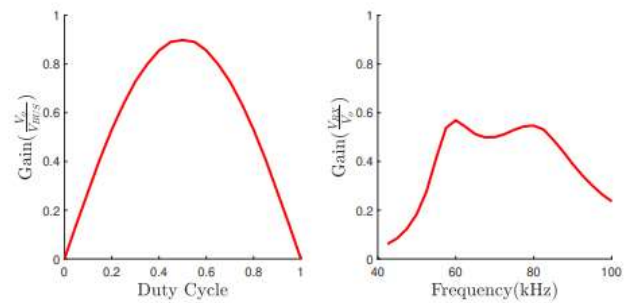

(a) Duty cycle-gain characteristic of IPT at 80 kHz. (b) Frequency-gain characteristic of IPT ($D = 0.5$).

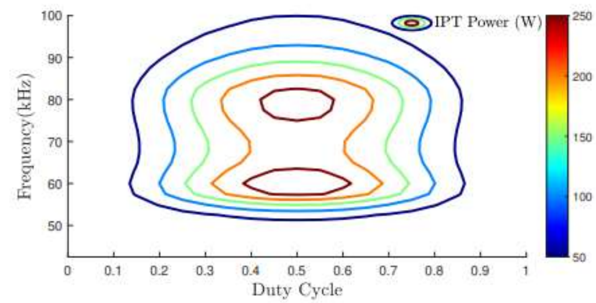

(c) The iso-power lines of IPT through duty cycle and frequency.

Experimental Results- WPT System Validation

	Design values	Measured values
Transmitter inductance	204μH	205μH
Receiver inductance	52μH	51μH
Mutual inductance	41μH	40μH

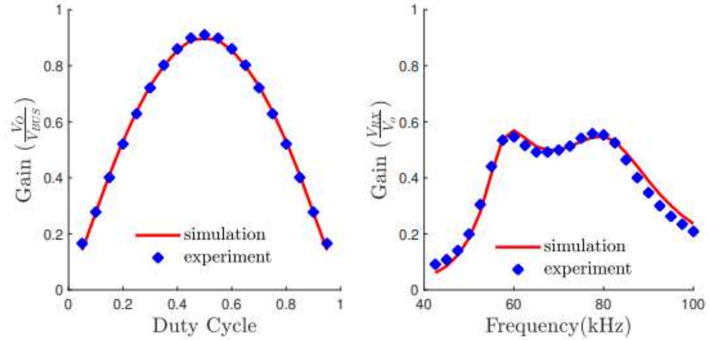

(a) Duty cycle-gain characteristic of WPT at 80 kHz. (b) Frequency-gain characteristic of WPT (D = 0.5).

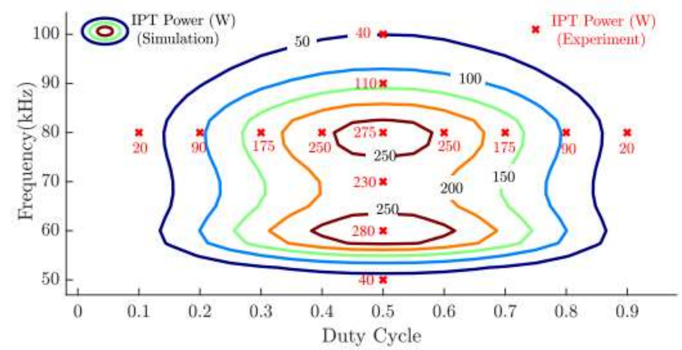

Experimental Results - Concurrent Operation

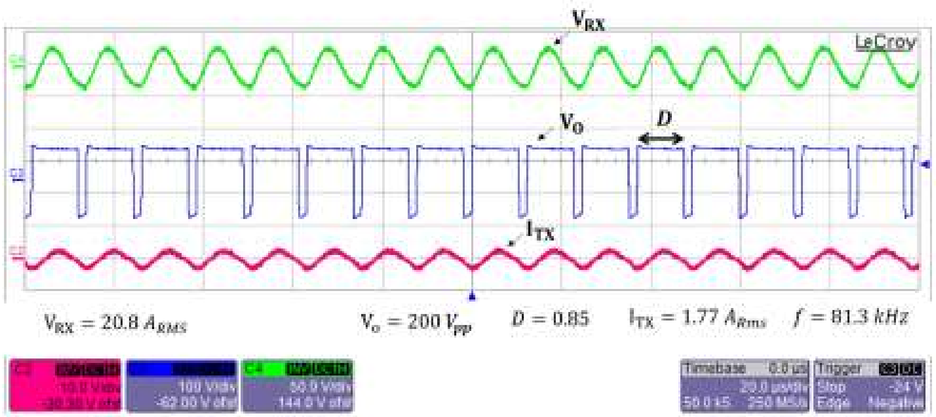

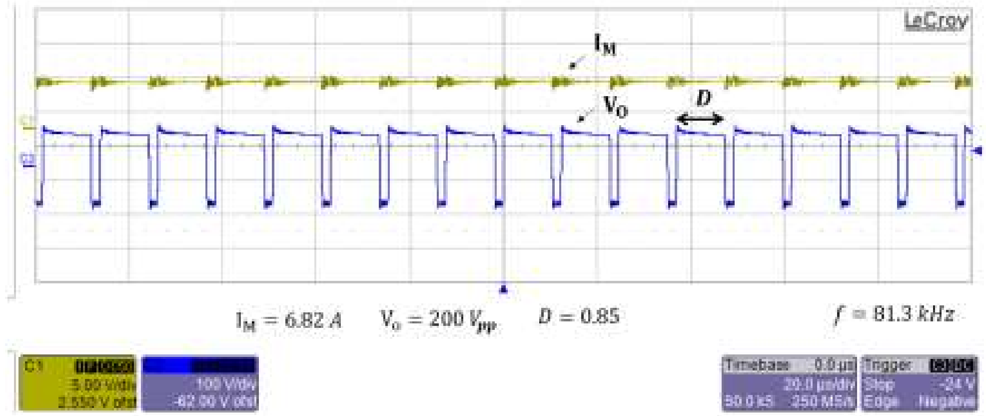

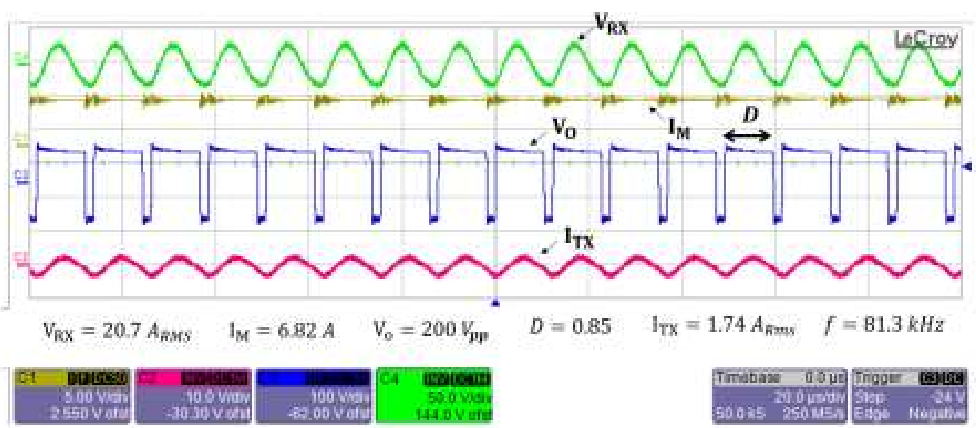

METU POWER LAB

Experimental Results – Loss and Efficiency

Operation	Input Power (W)	Drive Losses (W)	Converter Ouput Power (W)	Efficiency (%)
Only IPT	67.6	7.3	60.3	89.2
Only Motor	457.1	12.8	444.3	97.2
IPT and Motor	522.2	14.1	508.1	97.3

Experimental Results – Transient Load Changes

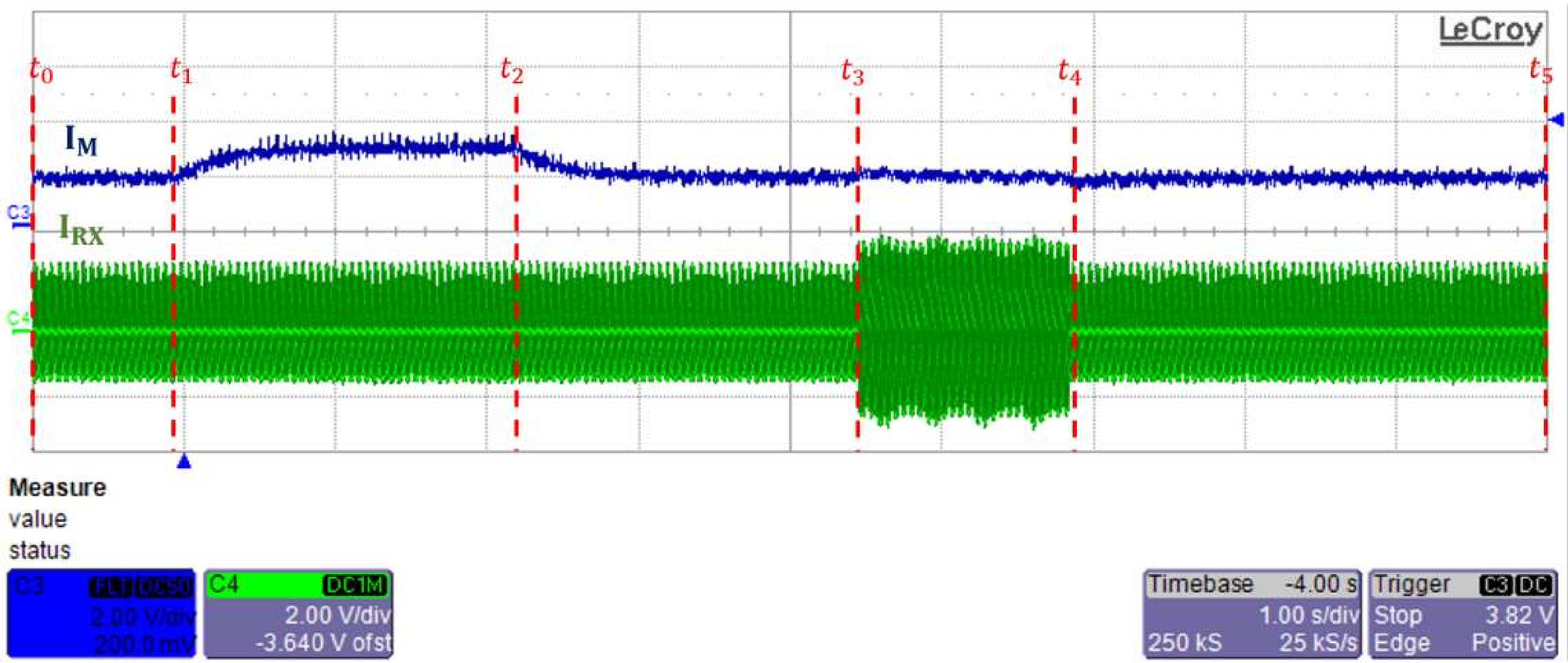

Experimental Results – Different Operating Conditions

	Cases						
	A	**B**	**C**	**D**	**E**	**F**	**G**
Frequency (kHz)	95	90	90	95	90	90	97.5
Duty Cycle	0.6	0.75	0.75	0.6	0.6	0.6	0.5
Load Torque (N.m)	0.24	0.27	0.37	0.21	0.21	0.17	-
Motor Power (W)	125	179	244	109	110	89	-
IPT Power (W)	50	51	51	50	90	90	52.7

Outline

System Overview and Experimental Setup

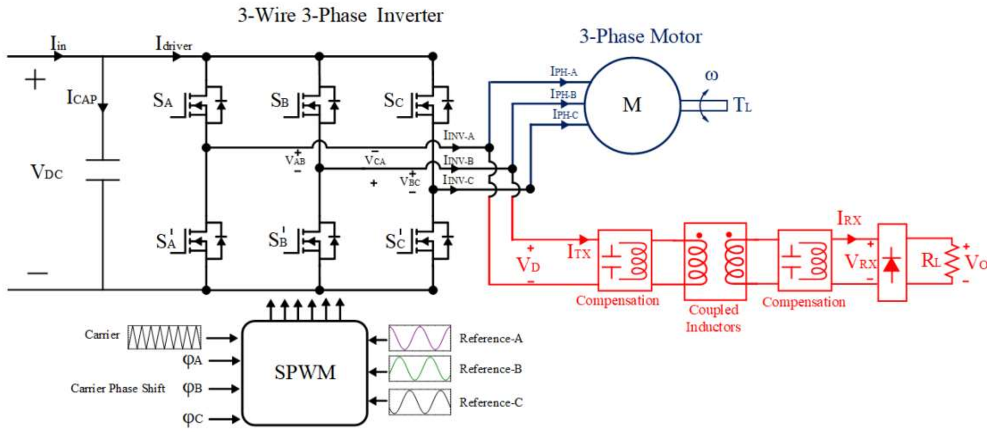

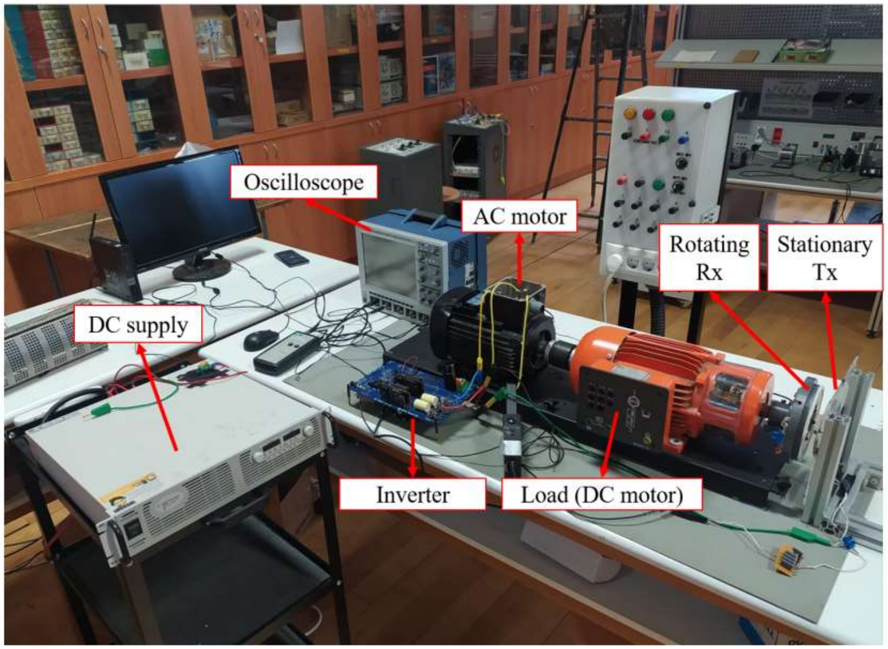

Ratings

DC-link voltage (V_{DC})	100 V
Modulation index (m_a)	0 – 1
Motor rated power (P_{motor})	500 W
Carrier-phase-shift range (Φ_{CPS})	30° – 60°
WPT-CSR output voltage (V_{OUT})	15 V_{RMS}
WPT-CSR input voltage (V_D)	30 V_{RMS}
WPT-CSR rated power ($P_{WPT-CSR}$)	24 W

Experimental Results- Carrier Phase Shift Validation

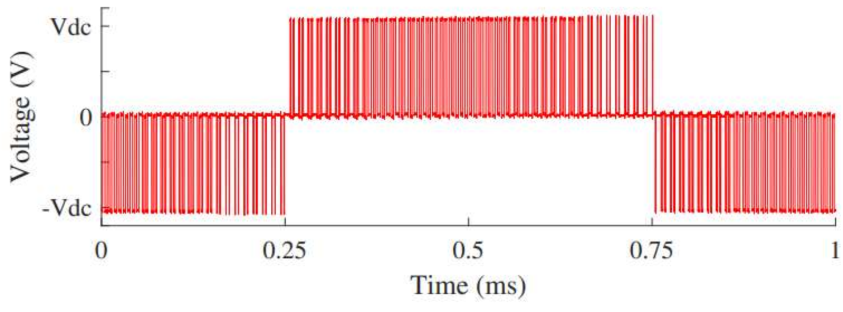

(a) $\phi_{CPS} = 0^o$

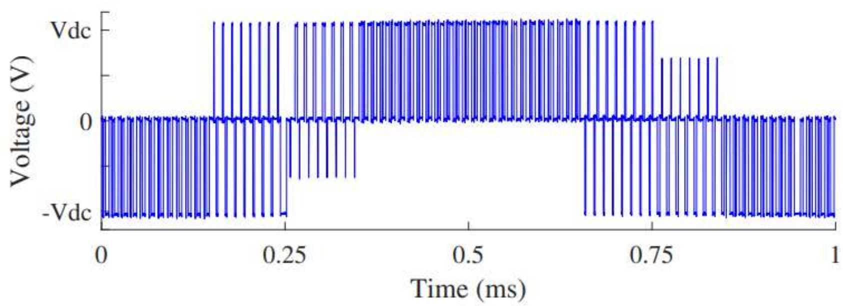

(b) $\phi_{CPS} = 47.5^o$

		A_{INV} $(\hat{V}_{ll}/V_{dc})$			
		at $\mathbf{f_o}$	at $\mathbf{f_l}$	at $\mathbf{f_s}$	at $\mathbf{f_h}$
$\mathbf{m_a = 0.6}$, $\boldsymbol{\phi_{CPS} = 0}$	**Theoretical**	0.519	0.113	0	0.113
	Experimental	0.532	0.110	0.011	0.115
	Error	2.5%	2.6%	-	1.7%
$\mathbf{m_a = 0.6}$, $\boldsymbol{\phi_{CPS} = 47.5^o}$	**Theoretical**	0.519	0.130	0.405	0.077
	Experimental	0.537	0.127	0.414	0.084
	Error	3.4%	2.3%	2.2%	9.1%

Wireless Power Transfer System Design

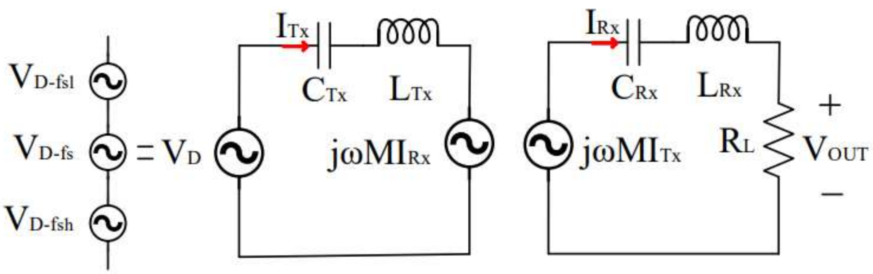

$$\omega_{rl} = \omega_r \sqrt{\frac{1}{1+k}}$$

$$\omega_{rh} = \omega_r \sqrt{\frac{1}{1-k}}$$

$$A_{WPT} = \left| \frac{V_{OUT}}{V_{IN}} \right|$$

$$\frac{dA_{WPT}}{dR_L} = 0$$

$$L_{Rx} = \frac{Q_{Rx} R_L}{\omega_{rh}} \longrightarrow A_{WPT(\omega_{rh})} = \left| \sqrt{\frac{L_{Rx}}{L_{Tx}}} \right| \longrightarrow L_{Tx} = \frac{L_{Rx}}{A^2_{WPT(\omega_{rh})}}$$

$$\downarrow$$

$$C_{Tx} = \frac{1}{\omega_r^2 L_{Tx}} \qquad C_{Rx} = \frac{1}{\omega_r^2 L_{Rx}} \longleftarrow M = k\sqrt{L_{Tx} L_{Rx}}$$

Wireless Power Transfer System Design

Initial/Choosen Parameters	Values	Derived Parameters	Values
P_{rated}	24 W	A_{WPT}	0.5
V_D	30 V_{RMS}	R_L	9.3 Ω
V_{out}	15 V_{RMS}	L_{Rx}	50 μH
f_{rh}	85 kHz	L_{Tx}	200 μH
Q_{Rx}	2.9	M	40 μH
k	0.4	f_r	65.85 kHz
		C_{Tx}	29.2 nF
		C_{Rx}	117 nF

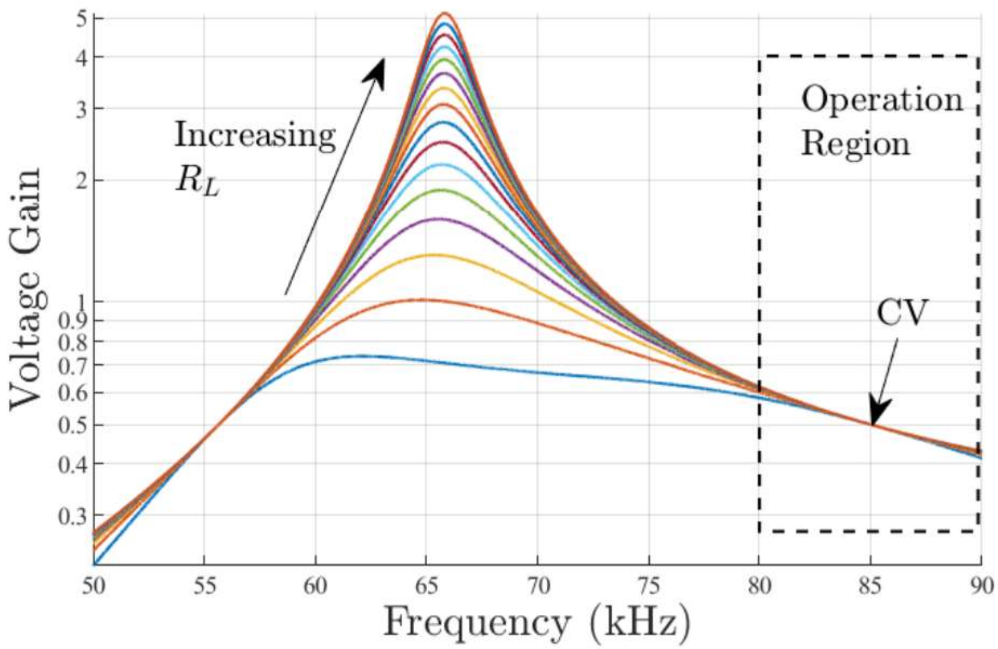

Experimental Results- WPT System Validation

	Design values	Measured values
Transmitter inductance	204μH	205μH
Receiver inductance	52μH	51μH
Mutual inductance	41μH	40μH

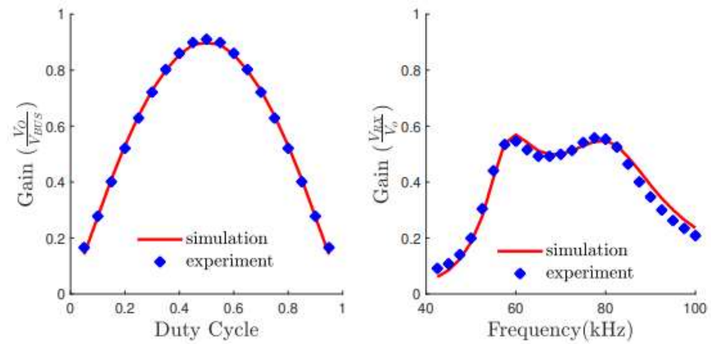

(a) Duty cycle-gain characteristic of WPT at 80 kHz. (b) Frequency-gain characteristic of WPT (D = 0.5).

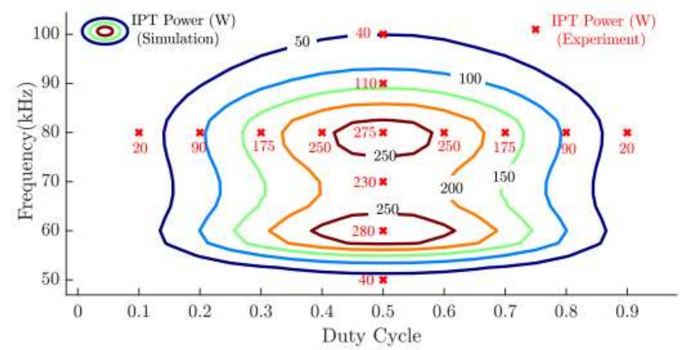

Experimental Results - Concurrent Operation

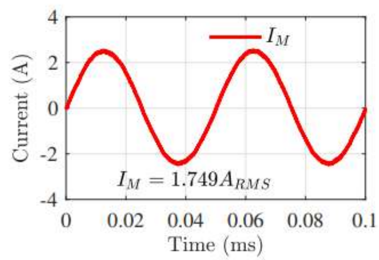

(a) Only motor operation.

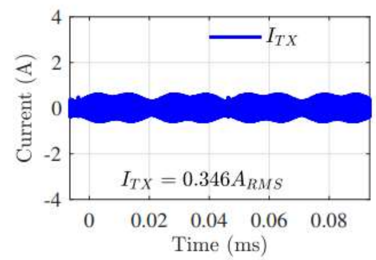

(b) Only WPT operation.

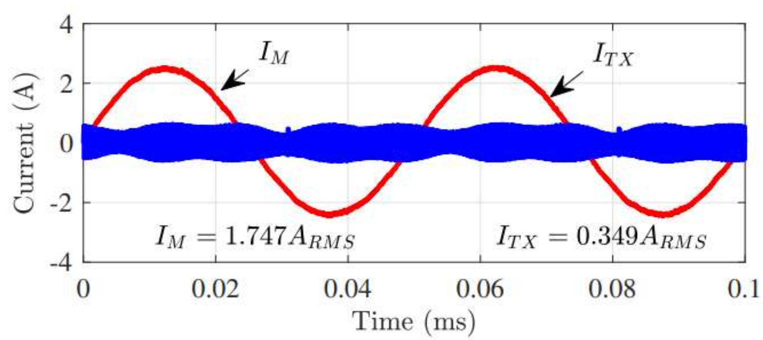

(c) Concurrent operation of motor and WPT.

Experimental Results – Variable Carrier Phase Shify

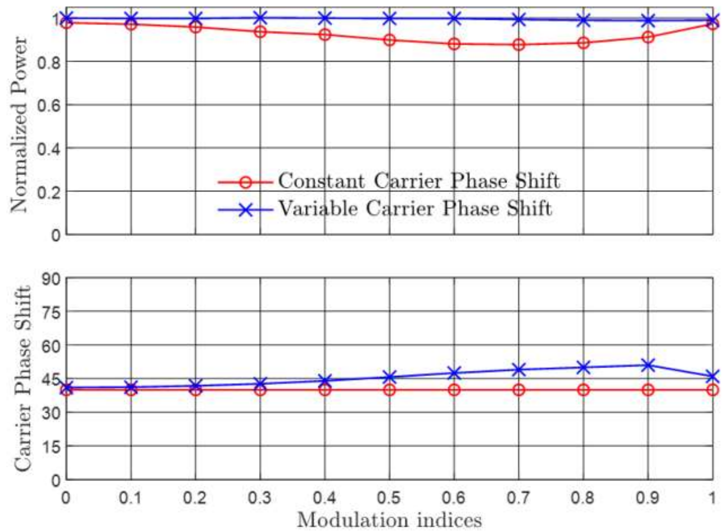

Modulation index (m_a)	0	0.1	0.2	0.3	0.4	0.5	0.6	0.7	0.8	0.9	1
Phase shift ($\theta_{\mathbf{an}}$) (Theoretical)	41	41	41.2	42.4	44.1	46.0	48.2	50.3	51.9	52.0	46
Phase shift ($\theta_{\mathbf{exp}}$) (Experimental)	41	41.2	41.8	42.7	44	45.7	47.5	49	50	51	46

Experimental Results – Transient Load Changes

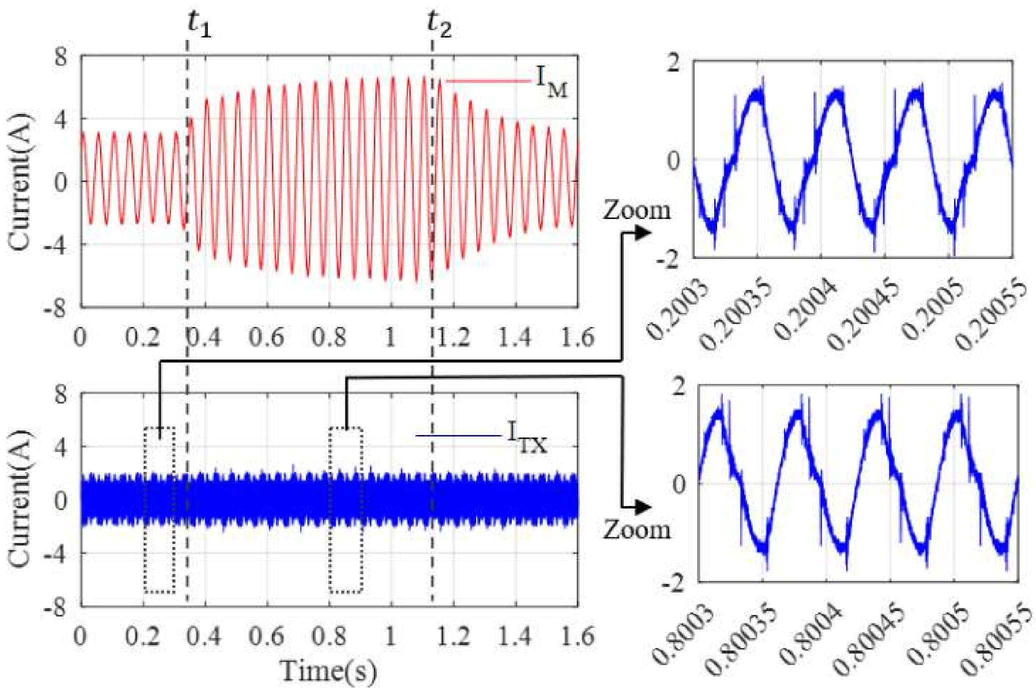

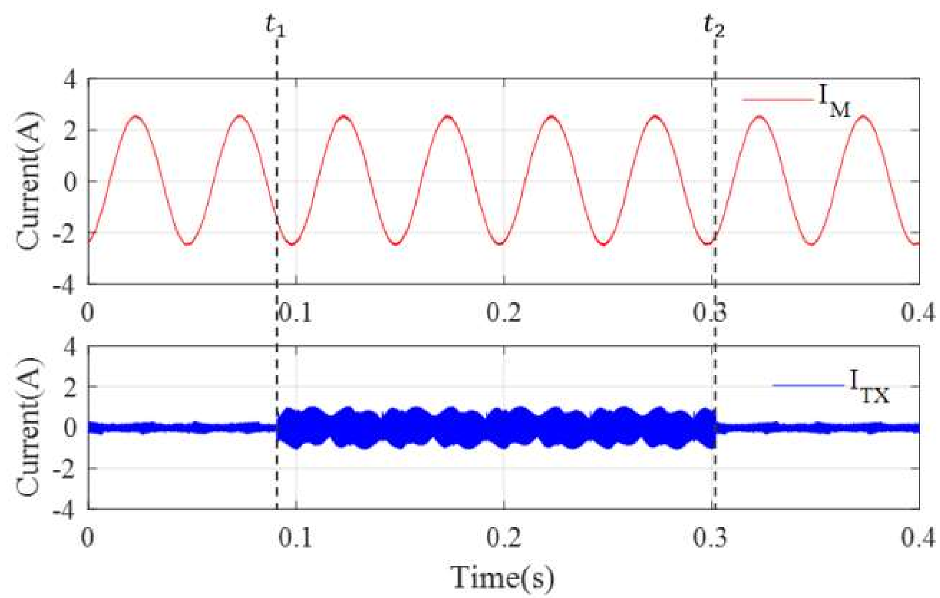

Outline

1. Aim of Study
2. Inductive Power Transfer System Basics
3. Theory Of Operations
4. Implementation for DC Motor
5. Implementation for AC Motor
6. **Implementation for field excitation**
7. Conclusion

System Overview and Experimental Setup

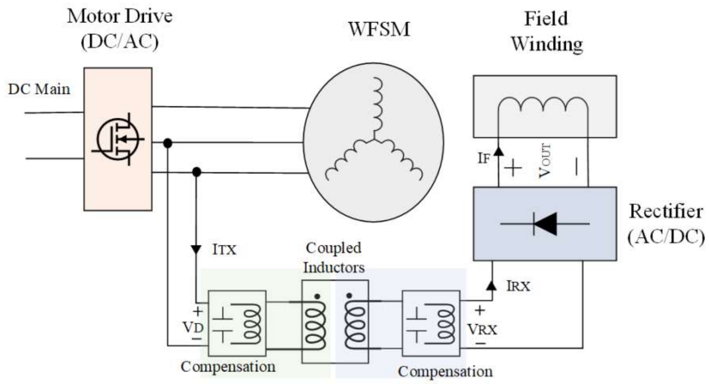

Ratings	
DC-link voltage (V_{DC})	100 V
Modulation index (m_a)	$0-1$
Field current (I_f)	5 A
Field resistance (R_L)	1.2Ω
The WPT system's rated output voltage (V_{OUT})	6 V
The WPT system's input voltage (V_D)	40 V_{RMS}
The WPT system's rated power ($P_{WPT-CSR}$)	30 W
Switching frequency (f_s)	60kHz

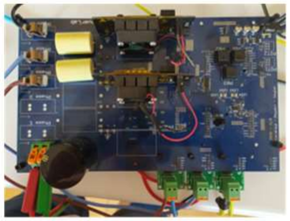

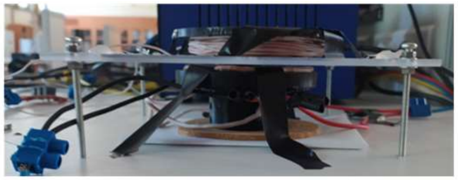

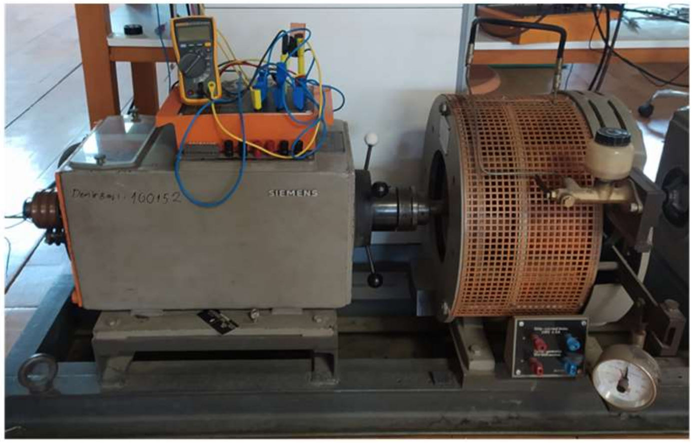

Wireless Power Transfer System Design

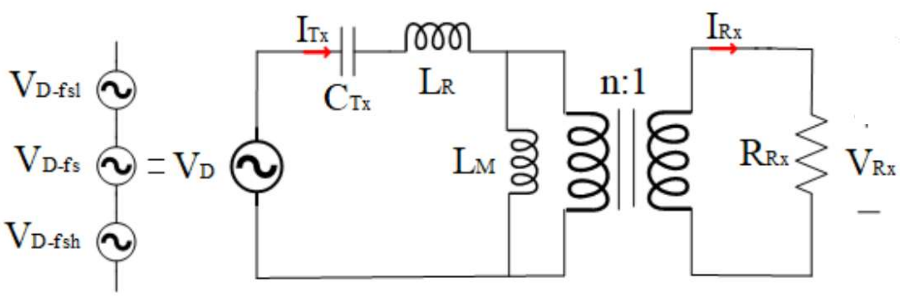

$$L_{Rx} = Q\frac{R_{Rx}}{\omega_r} \longrightarrow n = k\sqrt{\frac{L_{Tx}}{L_{Rx}}} \longrightarrow L_{Tx} = \frac{n^2}{k^2}L_{Rx}$$

$$n = \frac{V_D}{V_{Rx}}$$

$$C_{Tx} = \frac{1}{\sqrt{\omega_r^2 L_R}}$$

Initial/Choosen Parameters	Values	Derived Parameters	Values	Experimental Values
P_{rated}	30 W	V_{Rx}	7.56	-
V_D	40 V_{RMS}	R_{Rx}	0.97 Ω	-
V_{OUT}	6 V_{DC}	n	5.95	-
f_{rh}	60 kHz	L_{Tx}	1510 μH	-
Q_{Rx}	2.5	L_{Rx}	6.5 μH	-
k	0.7	M	42 μH	-
R_L	1.2 Ω	C_{Tx}	6.7 nF	-

Experimental Validation- Carrier Phase Shift

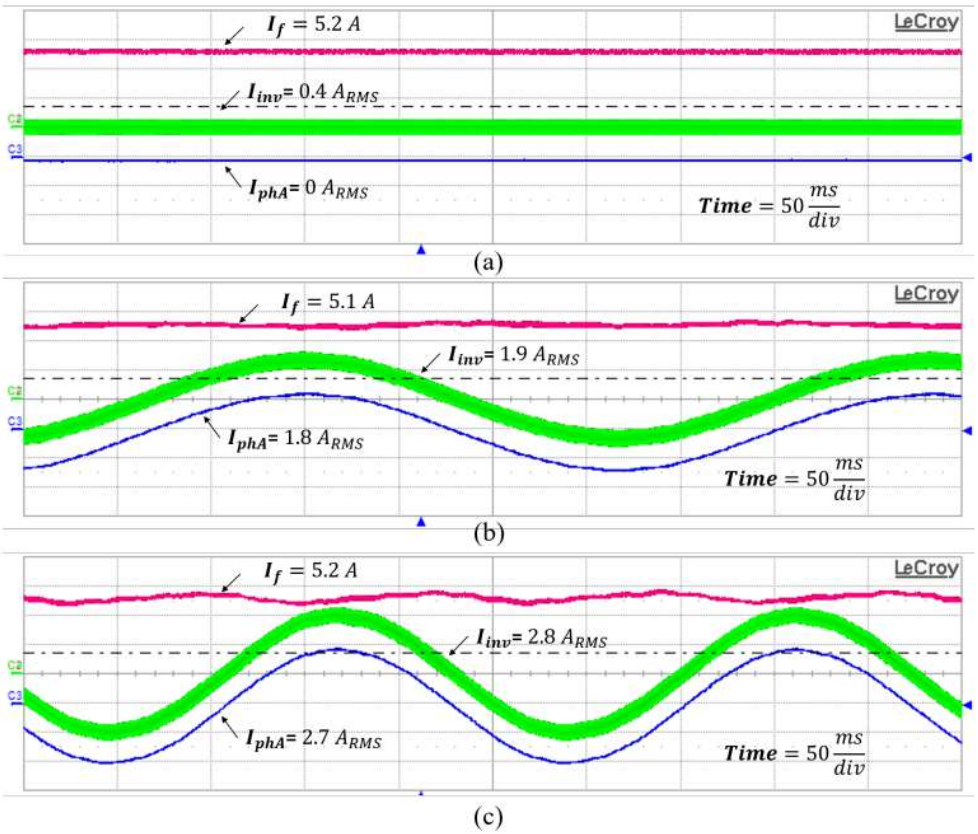

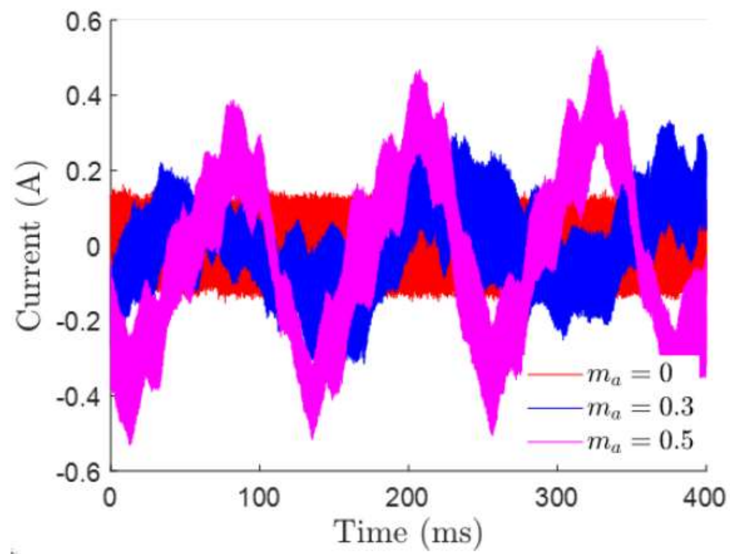

New real-time algorithm

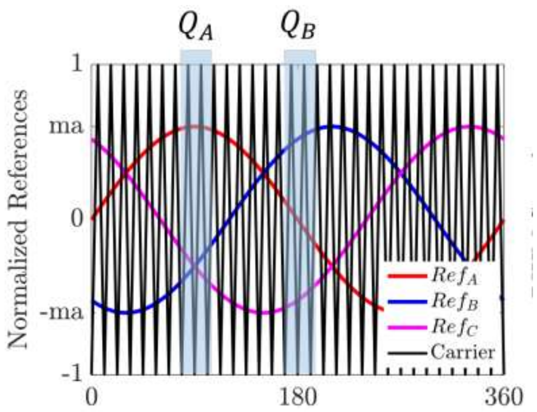

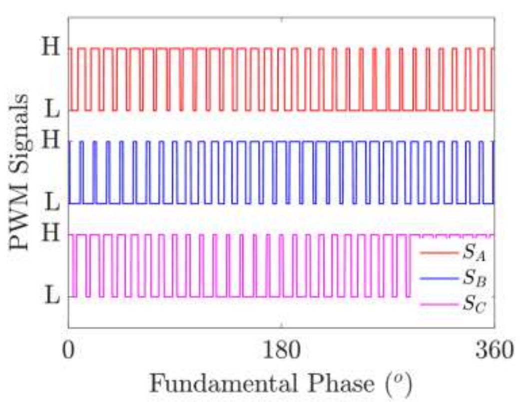

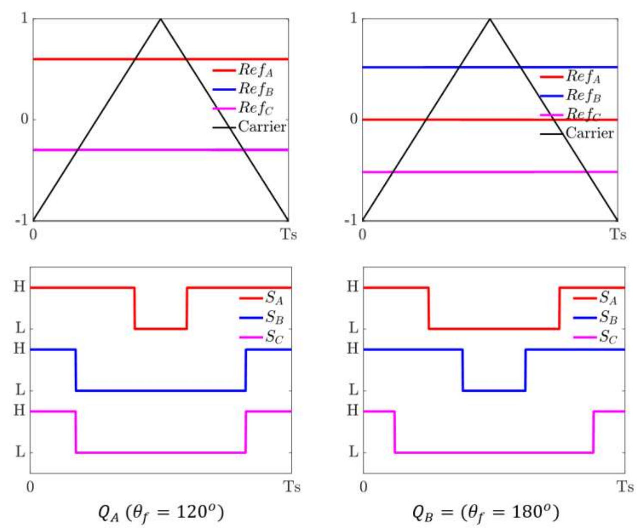

$$D_A = \frac{1 + m_a sin(\theta_f)}{2}$$

$$D_B = \frac{1 + m_a sin(\theta_f - 120)}{2}$$

$$D_C = \frac{1 + m_a sin(\theta_f + 120)}{2}$$

$$S(t) = \mathrm{D} + \sum_{k=1}^{\infty} \frac{2}{\mathrm{k}\pi} \sin(\mathrm{k}\pi\mathrm{D})\cos(2\pi\mathrm{k}\mathrm{f_s}\mathrm{t} + \mathrm{k}\phi_C)$$

New real-time algorithm

$$S_A(t)^{f_s} = \frac{2}{\pi} sin(\pi D_A) cos(2\pi f_s t + \phi_{C-A})$$
$$S_B(t)^{f_s} = \frac{2}{\pi} sin(\pi D_B) cos(2\pi f_s t + \phi_{C-B})$$
$$S_C(t)^{f_s} = \frac{2}{\pi} sin(\pi D_C) cos(2\pi f_s t + \phi_{C-C})$$

$$\begin{aligned} S_{AB}(t)^{f_s} &= S_A(t)^{f_s} - S_B(t)^{f_s} \\ &= \frac{2}{\pi} sin(\pi D_A) cos(2\pi f_s t + \phi_{C-A}) \\ &\quad - \frac{2}{\pi} sin(\pi D_B) cos(2\pi f_s t + \phi_{C-B}) \end{aligned}$$

$$\hat{S}_{AB_{f_s}} = \frac{2}{\pi} \sqrt{\begin{array}{c} sin(\pi D_A)^2 + sin(\pi D_B)^2 \\ -2(sin(\pi D_A)(sin(\pi D_B) cos(\phi_A - \phi_B) \end{array}}$$

New real-time algorithm

$$\frac{2}{\pi}|sin(\pi D_A) - sin(\pi D_B)| < \hat{S}_{AB_{fs}} < \frac{2}{\pi}|sin(\pi D_A) + sin(\pi D_B)|$$

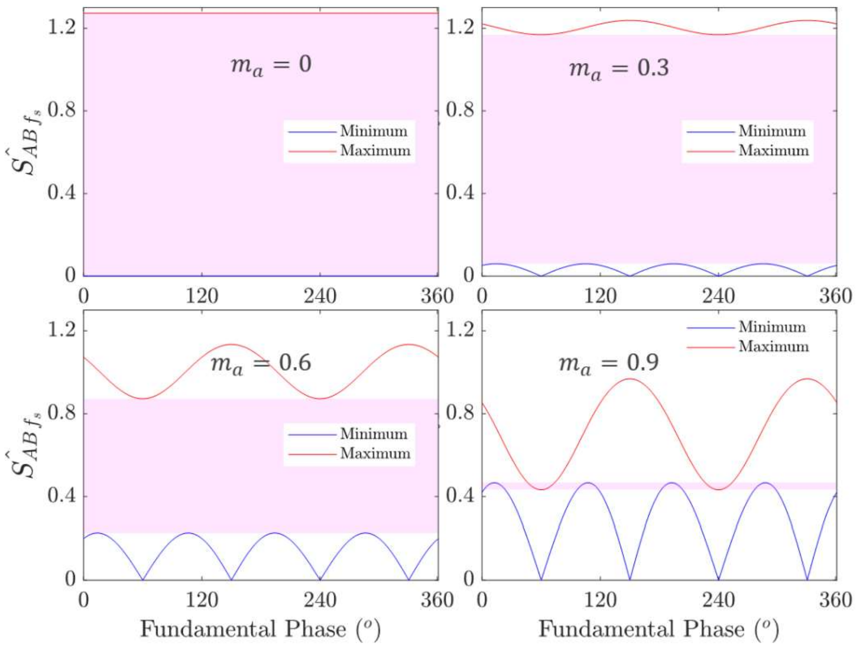

$\hat{S}_{AB_{fs}} = 0.43$!

$$\phi_{C-A} - \phi_{C-B} = acos\left[\frac{sin(\pi D_A)^2 + sin(\pi D_B)^2 - (\frac{\pi}{2}\hat{S}_{AB_{fs}})^2}{2sin(\pi D_A)sin(\pi D_B)}\right]$$

Experimental Validation- Carrier Phase Shift

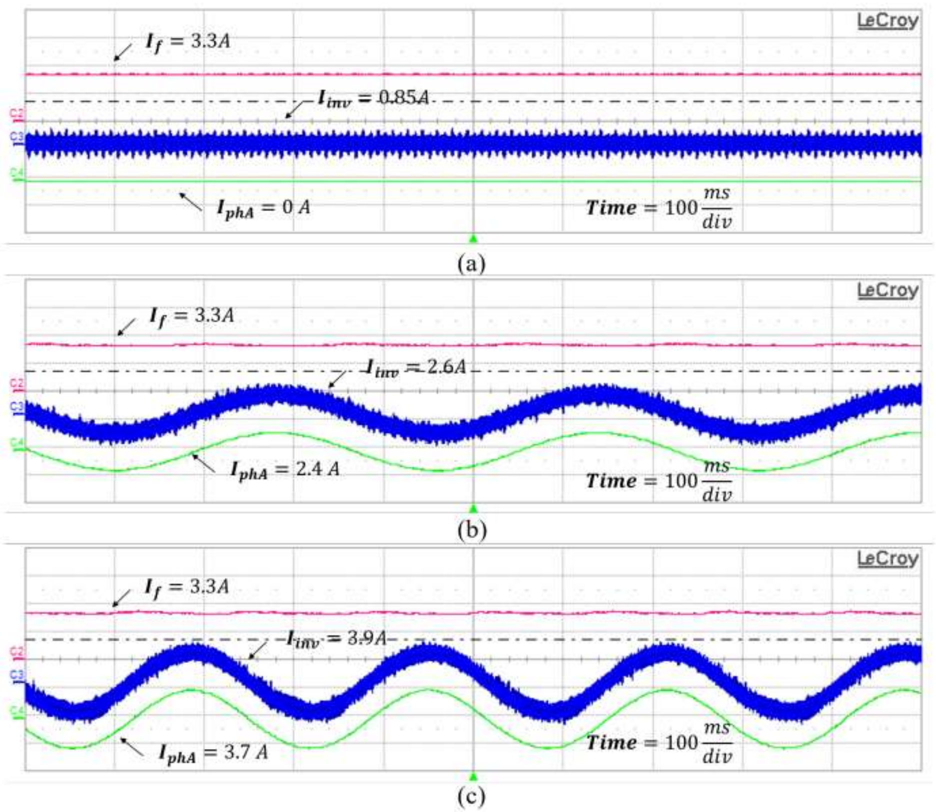

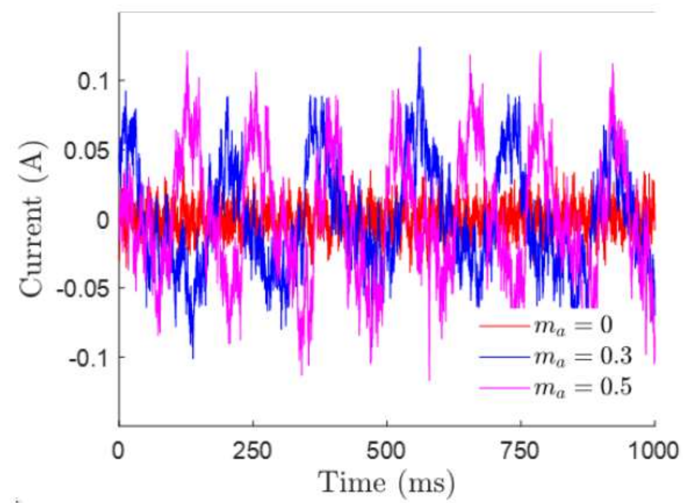

Outline

Performance Comparisons

Performance Metrics	Retrieved from [78]				The Proposed System
	Slip Rings	Brushless Exciters	Inductive Couplers	Capacitive Coupler	
Maintanance	Yes	No	No	No	No
Speed Sensitivity	Yes	Possible	No	Possible	No
Scalability	Diffucult	Easy	Possible	Possible	Difficult
Power Output	DC	DC	AC	AC	AC
Power Source	External DC	Shaft	External AC	External AC	Internal AC
Size	Small	Large	Medium	Medium	Medium

METU POWER LAB

Performance Comparisons

	[79]	[78]	[20]	[80]	[21]	[22]	[23]	[24]	[69]	[25]	[81]	This work
Frequency (kHz)	5	$>$650	250	100	848	50	1000	50	82.6	50	585	65
Power (W)	300	340	300	1000	100	231	10	500	3000	1000	10	50
Topology	RT	CPT	IPT	RT	CPT	IPT	IPT	IPT	IPT	IPT	IPT	IPT
Airgap (mm)	0.5	0.081	18	<2	0.125	70	2	-	10	0.6	10	10
Diameter (mm)	171	76.2	120	-	160	95	46	100	100	-	50	110
Efficiency (%)	85	85	92-95	90	94	>82	80	>80	92	>95	81	89
Additional converter	Yes	Yes	Yes	Yes	Yes	Yes	Yes	Yes	Yes	Yes	Yes	**No**

	Transfer Channels	Converter Numbers (Tx)	Offline Algortihm	Operating Frequency
[40]	1	1	Not Required	$\geq f_s$
[41]	2	2	Not Required	f_s
[42]	2	1	Required	$\leq f_s$
[44]	4	1	Not Required	$< f_s$
This work	2	1	Not Required	$= f_s$

Contributions

1. A cost-efficient and simple-to-implement contactless slip ring is introduced.
2. For DC motor drives, a multi-frequency approach is presented to implement with a conventional DC motor PWM technique.
3. An independent control scheme, which comprises frequency and duty cycle control, is proposed for concurrent DC and high-frequency AC power transfer to the motor and rotating loads, respectively.
4. For AC motor drives, a multi-frequency approach is presented to implement with a conventional AC motor PWM technique.
5. An independent control scheme, which comprises carrier phase shift and modulation index control, is proposed for concurrent low-frequency AC and high frequency AC power transfer to the motor and slip rings, respectively.
6. For field excitation of the synchronous motors, a brushless slip ring is proposed to directly integrate into the motor drive with light-weight on the rotating side.
7. A novel real-time carrier-phase-shift calculation algorithm embedded in the motor control loop is developed to avoid low-frequency ripples stemming from the sideband harmonics.

Future Works

1. Improved coil design.
2. Capacitorless (Light-weight rotating side) WPT topologies.
3. Multi-phase WPT system.
4. Closed loop control, and current estimation algorithms.

METU Power Lab

Thanks!